applied sciences

MDPI

Systematic Review

An Explicit Review and Proposal of an Integrated Framework to Improve Adaptive Front–Rear Brake Force Distribution in Electric Commercial Vehicles

Abdallah Yousef Aldaher [1,2,3], Alex Justice Frimpong [1,4], Ebaa Khaled Mohammed Matar [1,2], Jamshid Valiev Fayzullayevich [1,2], Haoting Wei [1,2] and Gangfeng Tan [1,2,*]

[1] School of Automotive Engineering, Wuhan University of Technology, Wuhan 430070, China; abdallahaldaher@whut.edu.cn (A.Y.A.); alexua45@whut.edu.cn (A.J.F.); ebaamatar@whut.edu.cn (E.K.M.M.); jamshidvaliev@whut.edu.cn (J.V.F.); 362435@whut.edu.cn (H.W.)
[2] Suizhou-Wuhan University of Technology Industry Research Institute, Suizhou 441300, China
[3] Vocational Education (BTEC), Jordanian Ministry of Education, Amman 11118, Jordan
[4] Department of Automotive and Agricultural Mechanization Engineering, Kumasi Technical University, Kumasi 00233, Ghana
* Correspondence: auto_nova@whut.edu.cn; Tel.: +86-18995570176

Featured Application

Improving brake safety and efficiency in electric commercial vehicles.

Abstract

Adaptive brake force distribution (BFD) is critical for the safety and efficiency of electric commercial vehicles (ECVs), yet the integration of thermal constraints, real-time control, and stability requirements remains fragmented. Following PRISMA 2020, a systematic search in IEEE Xplore and Web of Science (2016–2026) was performed, yielding 156 core studies classified into five thematic groups: fundamentals, MPC-based control, PSO, integrated frameworks, and validation methods. The analysis reveals a tripartite fragmentation: 27 MPC studies neglect thermal constraints; 22 PSO studies lack real-time adaptability; 52 studies target commercial vehicles, but none validate front–rear redistribution under concurrent thermal and stability constraints. Only two studies address thermal-aware distribution, and seven consider pneumatic delay compensation. Publication volume accelerates, indicating rising interest. The literature treats thermal management, real-time redistribution, and stability-constrained control as separate problems, leaving a critical gap: online correction of the ideal distribution curve under coupled thermal-stability constraints for ECVs is absent. To fill this gap, a hierarchical MPC-PSO framework is proposed, where PSO (1–5 Hz) adaptively tunes MPC weights based on vehicle state, and MPC (20–50 Hz) executes optimal control integrating regenerative, magnetic, and eddy current braking. This research aims to achieve two main objectives: to propose a new integrated framework that addresses the overlooked interrelationship between the stability constraints of ECVs and thermal constraints and to systematically reveal the state of integrative constraints on adaptive brake force distribution in electric commercial vehicles, with a focus on real-time control and stability requirements.

Keywords: adaptive brake force distribution; model predictive control; particle swarm optimization; thermal-stability coupling; electric commercial vehicles; regenerative braking

Check for updates

Academic Editor: Ján Dižo

Received: 11 May 2026
Revised: 4 June 2026
Accepted: 5 June 2026
Published: 8 June 2026

Copyright: © 2026 by the authors. Licensee MDPI, Basel, Switzerland. This article is an open access article distributed under the terms and conditions of the Creative Commons Attribution (CC BY) license.

1. Introduction

The present review defines the research problem and its context, identifies gaps in the literature, highlights the threefold fragmentation among thermal constraints, stability constraints, and real-time control, and presents the aims, contributions, novelty, and the need for an adaptive brake distribution system in electric commercial vehicles.

1.1. Motivation and Problem Statement: Safety, Efficiency, and Fragmentation in Electric Commercial Vehicles

The braking system is one of the most safety-critical subsystems that faces unresolved fragmentation in balancing thermal, real-time, and stability constraints during adaptive front–rear brake force distribution. Its fundamental objective of decelerating the vehicle while maintaining directional stability becomes substantially more complex in the context of electrification, where friction braking must be coordinated with regenerative torque from electric motors [1–3]. The allocation of braking effort between the front and rear axles, commonly expressed as the ideal brake force distribution curve (also referred to as the I-curve or the β-line), defines the boundary along which both axles lock simultaneously under a given deceleration [4–6]. Departures from this ideal locus, whether upward or downward in the front-to-rear force ratio, degrade either tire adhesion utilization, energy recovery efficiency, or both [7–9].

In conventional braking systems, the distribution is fixed through proportioning valve geometry [6,10]. The introduction of brake-by-wire (BBW), electro-hydraulic brake (EHB), and electro-mechanical brake (EMB) actuators removes this constraint and opens the possibility of adaptive, real-time redistribution [11–13]. For passenger electric vehicles (EVs), this capability has been leveraged primarily to maximize regenerative energy recovery while maintaining stability [5,8,14]. However, commercial vehicles ranging from medium-duty delivery trucks to heavy articulated lorries operate under highly variable loading conditions and road surfaces [10,15–17].

Three specific challenges distinguish commercial vehicle brake force distribution from passenger vehicle applications. First, the mass variation between laden and unladen states can exceed 150%, fundamentally altering the ideal distribution curve and the dynamic weight transfer during braking [18,19]. Second, sustained braking on long descents or in urban stop-and-go traffic induces thermal loading that degrades the friction coefficient, increases brake fade risk, and shifts the effective distribution away from the ideal curve [1,20,21]. Third, pneumatic brake actuators ubiquitous in heavy commercial vehicles due to their high force capacity introduce time delays (50–150 ms) and nonlinear pressure–force characteristics that complicate real-time control [22–24].

The electrification of commercial vehicles amplifies these challenges while introducing new opportunities. Electric commercial vehicles (ECVs) can recover braking energy through motor generators on one or both axles, but the distribution of regenerative versus friction braking must respect motor torque limits, battery charge acceptance, and thermal constraints on both the electric drivetrain and the friction brakes [25–27]. The coupling between energy recovery objectives and stability constraints creates a multi-objective optimization problem that cannot be solved by fixed distribution strategies [28,29].

Despite an expanding body of literature on regenerative braking, model predictive control (MPC), and particle swarm optimization (PSO), no unified framework has been established that dynamically corrects the ideal brake force distribution curve in real time under concurrent thermal loading and longitudinal stability constraints [30–32]. A preliminary survey of the literature reveals a structural tripartite fragmentation:

Fragmentation 1: Thermal management versus real-time control. Studies addressing brake thermal dynamics typically focus on offline design optimization (e.g., cooling system

sizing, material selection) or post hoc thermal analysis, but do not integrate thermal-state feedback into the real-time brake force distribution controller [1,20,21]. Conversely, real-time control studies assume constant friction coefficients and omit thermal constraints from the MPC formulation [33–35].

Fragmentation 2: Stability control versus energy optimization. MPC-based studies prioritize vehicle stability (yaw rate tracking, sideslip angle limitation) and formulate the brake force distribution as a constrained optimal control problem, but systematically omit energy recovery objectives and treat regenerative braking as a secondary, decoupled problem [9,36,37]. PSO-based studies optimize energy recovery parameters (regenerative braking intensity, front–rear distribution ratio) offline or in quasi-static scenarios, but lack the real-time adaptability and constraint satisfaction guarantees required for safety-critical control [16,38,39].

Fragmentation 3: Passenger vehicles versus commercial vehicles. The majority of studies focus on EVs with symmetric axle loads, hydraulic brakes, and moderate mass variation [17,40,41]. Commercial vehicle-specific challenges, such as pneumatic actuator delays, extreme mass variation, thermal loading from sustained braking, and regulatory compliance with ECE-R13, are underrepresented in the literature [22,24,42].

This tripartite fragmentation creates a critical research gap: the absence of a unified, real-time controller that corrects the ideal brake force distribution curve under coupled thermal-stability constraints for electric commercial vehicles. Addressing this gap requires a control architecture that integrates MPC for stability-constrained optimal control, PSO for adaptive parameter tuning, thermal-state estimation for fade compensation, and pneumatic actuator modeling for delay compensation [7,43]. This highlights the need to diversify braking systems, such as regenerative braking, ECR, magnetic clutch, or magnetic brake, to achieve overall safety, optimal and efficient component sustainability and integration, and to maintain optimal braking and stability, especially under difficult conditions, long operating hours, and high loads, thus ensuring longevity and safety.

This research aims to address the safety and efficiency gap resulting from the fragmented treatment of real-time stability and thermal constraints when distributing the braking force in electric vehicles. Through the aforementioned threefold fragmentation, critical research gaps emerged that directly justify this need: (1) the lack of immediate adaptation to changing load conditions (loaded/unloaded); (2) the absence of real-time thermal-stability correlation; (3) the neglect of compliance with the ECE-R13 standard in adaptation strategies; and (4) the lack of validation of the redistribution between the two axes under concurrent stability and thermal constraints. These gaps motivate the objectives and innovations presented in the following two Sections 1.2 and 1.3.

1.2. Research Objectives and Contributions

This systematic literature review addresses the identified research gaps through six specific objectives. First, it organizes the literature into a coherent thematic taxonomy spanning fundamentals (ideal curve theory, ECE-R13), MPC-based control, PSO-based optimization, integrated frameworks, and validation methods. Second, it quantifies the prevalence of thermal constraints, commercial vehicle focus, MPC-PSO integration, and physical validation across the 156-study corpus. Third, it provides a structured methodological comparison of MPC and PSO formulations, constraint handling, prediction horizons, computational complexity, and validation environments through comparative tables. Fourth, it analyzes publication volume, vehicle type distribution, and methodological evolution from 2016 to 2026. Fifth, it delineates six critical research gaps (G1–G6) with severity scores and evidence-based justification. Sixth, it proposes a hierarchical MPC-PSO framework with a

three-layer architecture (PSO 1–5 Hz, MPC 20–50 Hz, actuation/monitoring) validated by a physical test rig.

The primary contribution of this review is the explicit identification and quantification of the tripartite fragmentation and the proposal of a unified hierarchical MPC-PSO framework.

Scientifically, this framework introduces a novel coupling of thermal-state estimation with real-time MPC-PSO, which has not been previously integrated for electric commercial vehicles. Practically, it offers a deployable control architecture that can be implemented on existing brake system hardware to mitigate thermal fade and maintain stability under different conditions. This work positions adaptive front–rear brake force distribution as a dynamic, control-oriented problem essential for the safety and commercial viability of electric commercial vehicles.

1.3. Novelty and Significance

The novelty of this review lies in three aspects. First, it is the first PRISMA 2020-compliant systematic review to explicitly target the intersection of adaptive brake force distribution, thermal constraints, and commercial vehicles. Second, it quantifies the structural fragmentation across 156 studies using a five-group taxonomy and six research gaps with severity scores. Third, it proposes a hierarchical MPC-PSO framework with a detailed test rig architecture, bridging the gap between theoretical control design and physical validation.

The significance of this work extends beyond academic contribution. The proposed framework addresses a critical safety and efficiency challenge in the electrification of commercial transportation, with direct implications for regulatory standards (ECE-R13), vehicle design (brake-by-wire architectures), and operational safety (thermal fade mitigation). As commercial EV adoption accelerates, the need for thermally aware, adaptive brake force distribution becomes increasingly consequential [44].

The scientific novelty lies in the real-time integration of thermal constraints into the online correction of the ideal brake force distribution curve, which is a problem identified in the reviewed literature. And the practical contribution is a hierarchical control architecture (PSO at 1–5 Hz for weight adaptation, MPC at 20–50 Hz for execution) that can be directly implemented on commercial vehicle electronic control units (ECUs) with existing sensor suites, enabling thermal fade compensation without additional hardware costs.

1.4. Paper Structure

The remainder of this paper is organized as follows. Section 2 describes the PRISMA 2020 methodology, including database selection, search strategy, inclusion/exclusion criteria, and quality assessment. Section 3 presents the thematic literature review organized into five groups: fundamentals, MPC-based control, PSO-based optimization, integrated frameworks, and validation methods. Section 4 analyzes six research gaps (G1–G6) with severity scores and evidence-based justification. Section 5 proposes the hierarchical MPC-PSO framework with a three-layer architecture and test rigor specification. Section 6 presents conclusions and policy implications.

2. Method for Literature Selection and Scope of Study

The methodology employed for literature selection and study classification is presented below.

2.1. Compliance with Prisma 2020 Standards

This systematic review adheres to the guidelines of the "Preferred Reporting Items for Systematic Reviews and Meta-analyses" (Prisma) of 2020 [45]. Due to the engineering focus of the topic, the review protocol was followed at Prospero. In addition to documenting the research strategy, inclusion/exclusion criteria and a data extraction protocol in advance,

according to the Prisma 2020 criteria, with a narrative critical review of the listed studies were used. The completed PRISMA 2020 checklist and the PRISMA 2020 abstract checklist are provided in Tables S1 and S2 in the Supplementary Materials.

2.2. Information Sources and Search Strategy

A systematic search was conducted using two electronic databases selected for their comprehensive coverage of the transportation engineering, control systems, and vehicle dynamics literature: IEEE Xplore Digital Library (coverage 1963–present, containing IEEE journals, conferences, and standards) and Web of Science Core Collection (coverage 1900–present, containing multidisciplinary journals indexed in SCI-EXPANDED). The search retrieved 1041 records from IEEE Xplore and 891 records from Web of Science. Boolean queries combining three concept groups, (1) brake force distribution, (2) control/optimization methods, and (3) vehicle type, were applied to titles, abstracts, and author keywords. The full query strings are provided below:

IEEE Xplore Query: ("brake force distribution" OR "braking force distribution" OR "front-rear brake" OR "brake torque distribution" OR "axle brake distribution") AND ("model predictive control" OR "MPC" OR "particle swarm" OR "PSO" OR "optimal control") AND ("electric vehicle" OR "commercial vehicle" OR "heavy vehicle" OR "truck" OR "bus").

Web of Science Query: ("brake force distribution" OR "braking force distribution" OR "front-rear brake") AND ("model predictive control" OR "particle swarm optimization" OR "MPC" OR "PSO") AND ("electric vehicle" OR "commercial vehicle" OR "heavy-duty vehicle" OR "truck" OR "bus").

The search was limited to the period 1 January 2016–1 March 2026 (a ten-year window for currency), English-language only, and peer-reviewed document types (journal articles and conference papers).

2.3. Eligibility Criteria

Inclusion and exclusion criteria were defined using the PICOS (Population, Intervention, Comparator, Outcome, Study Design) framework: Table 1 includes the specifications of inclusion and exclusion criteria of the studies:

Table 1. Inclusion and exclusion criteria and specifications of the studies.

Aspect	Description
Inclusion Criteria	1. Population (P): Commercial vehicles (trucks, buses, heavy-duty vehicles) or electric vehicles with front–rear braking systems. 2. Intervention (I): Adaptive or optimal brake force/torque distribution between front and rear axles. 3. Comparator (C): Fixed/static brake distribution, alternative control methods, or baseline performance. 4. Outcome (O): Braking performance (stopping distance, deceleration), stability (yaw rate, sideslip), thermal management, energy recovery. 5. Study Design (S): Peer-reviewed journal articles or conference papers with quantitative results. 6. Language: English only. 7. Year: 2016–2026 (10-year window).
Exclusion Criteria	1. Non-peer-reviewed thesis/dissertations quality and reproducibility concerns. 2. Patents: not primary research literature. 3. Non-braking focus (steering, suspension only) outside scope. 4. Non-English language: language accessibility. 5. No quantitative results: insufficient evidence quality. 6. Lateral-only brake distribution (left–right): scope limited to front–rear (longitudinal). 7. Pre-2016 publications: superseded by more recent methods. 8. Retracted papers: integrity concerns. 9. Duplicate records: identified via DOI and title matching with Zotero.

2.4. Selection Process and PRISMA Flow

The selection process followed the PRISMA 2020 four-stage workflow (identification, screening, eligibility, inclusion). A total of 1933 records were identified from IEEE Xplore (1041) and Web of Science (891). After removing 371 duplicate records (by DOI and title matching) and 3 retracted records (identified via Retraction Watch), 1562 unique records remained. Title and abstract screening excluded 201 off-topic records, leaving 1361 records. Full-text eligibility assessment further categorized 1202 records as supporting (indirectly relevant or background) and identified 156 core papers that fully met the inclusion criteria. These 156 core papers were included in the final synthesis. The complete PRISMA flow diagram is presented in Figure 1.

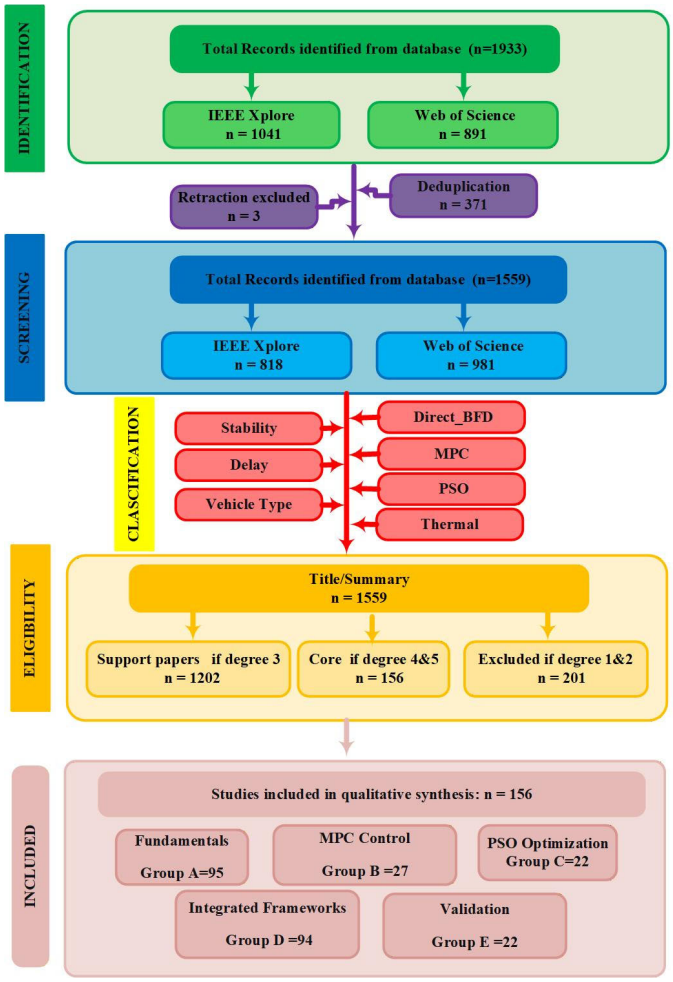


Figure 1. PRISMA 2020 flow diagram for the systematic literature review on adaptive front–rear brake force distribution in electric commercial vehicles. Note: Studies may belong to multiple thematic groups.

Other control and optimization techniques such as genetic algorithms (GAs), fuzzy logic, rule-based control, and reinforcement learning (RL) exist in the broader electric vehicle braking literature. However, these methods did not appear in the core set (score ≥ 8) for one or more of the following reasons: they lacked experimental or high-fidelity validation, omitted the coupled thermal-stability constraints, or did not focus on adaptive front–rear distribution for commercial vehicles. Consequently, the 27 MPC and 22 PSO studies represent the most methodologically rigorous and directly relevant evidence base for the gaps identified in this review. A comparative discussion of MPC/PSO versus other techniques is provided in Sections 3.2 and 3.3.

2.5. Data Extraction and Classification

For each of the 156 included studies, bibliographic metadata (authors, year, journal/conference, DOI), vehicle type, control method, constraint types (thermal, stability, delay, energy), validation level (simulation, hardware-in-the-loop, test rig, full vehicle), key contributions and limitations, and thematic group assignment were extracted into a structured spreadsheet. Based on their primary focus, the studies were classified into five thematic groups (A–E), with the understanding that a single study may belong to multiple groups. The occurrence counts per group are as follows: Group A (fundamentals): 95 studies; Group B (MPC-based control): 27 studies; Group C (PSO-based optimization): 22 studies; Group D (integrated frameworks): 94 studies; Group E (validation methods): 22 studies. These numbers represent occurrences (i.e., a study addressing multiple themes is counted in each relevant group). After resolving overlaps, the unique assignment of each study to a single primary group is summarized in Table 2, together with key topics and representative references.

Table 2. Unique classification of studies by primary thematic group (A–E).

Group	Theme	Key Topics	Representative Papers
A	Fundamentals	Ideal curve theory, BFD physics, dynamic axle load, regen friction blending, multi-axle dynamics, ECE R13	[5,8,15,46,47]
B	MPC-Based Braking Control	Linear/NMPC, adaptive MPC, force-based MPC, pneumatic delay, stability	[3,11,13,48–52]
C	PSO-Based Optimization	Offline PSO, multi-objective PSO, thermal-aware PSO, real-time PSO, hybrid variants	[30–32,39,53–57]
D	Integrated Frameworks	MPC PSO combined, hierarchical control, energy stability coupling, ECV strategies	[10,19,58,59]
E	Validation	Simulation, HIL testing, test bench, full-scale vehicle, co-simulation	[5,7,14,20–22,41,42,50,51,60–63]

For each group, the table lists key topics, representative references, and the number of studies uniquely assigned to that group based on their dominant contribution. A study may appear in more than one group in the occurrence counts, but here, each study is assigned to only one primary group. Overlaps are handled separately in the synthesis.

2.6. Quality Assessment and Risk of Bias

Each of the 1559 records was evaluated for methodological quality using a five-dimensional scoring system (0–2 points per dimension, maximum 10 points). The dimensions were: (1) model validity: whether the vehicle or brake model is validated against experimental data; (2) control design rigor: whether stability, optimality, and constraint satisfaction are demonstrated; (3) experimental validation: whether hardware-in-the-loop, test bench, or full-vehicle testing is performed; (4) reproducibility: whether parameters, equations, and methods are sufficiently detailed; and (5) commercial vehicle relevance: whether the study addresses heavy-duty or electric commercial vehicle-specific challenges. Based on their total score, studies were classified into three categories: core ($\geq$8 points; 156 records), supporting (6–7 points; 1202 records), and excluded ($\leq$4 points; 201 records). The excluded records were not considered further in the synthesis. Quality scores informed the weighting of evidence for the core and supporting studies. This classification is consistent with the PRISMA flow diagram (Figure 1). The thematic synthesis focused exclusively on the 156 core papers; supporting studies were used for contextualization.

3. Brake Force Distribution—Fundamentals and State of the Art

The following subsections present a thematic literature review structured into five groups (A–E) corresponding to the state of the art in brake force distribution.

3.1. Group A: Fundamentals of Brake Force Distribution and Ideal Curve Theory

The theoretical foundation of front–rear brake force distribution is established by the ideal distribution curve (I-curve), which defines the locus of front and rear brake forces that cause both axles to lock simultaneously under a given deceleration [4,6,64–66]. This curve is derived from the longitudinal dynamics of a two-axle vehicle under braking, considering static weight distribution, dynamic weight transfer, and tire–road adhesion limits [18,19].

The taxonomic structure of adaptive BFD for electric commercial vehicles is illustrated in Figure 2, which organizes the literature into five thematic groups (A–E) and highlights the relative prevalence of fundamental studies (Group A) compared to experimental validation (Group E). The radial hierarchy reinforces that fundamental BFD principles remain indispensable, yet their real-time adaptation under thermal and delay constraints—particularly for commercial vehicles—remains critically underexplored.

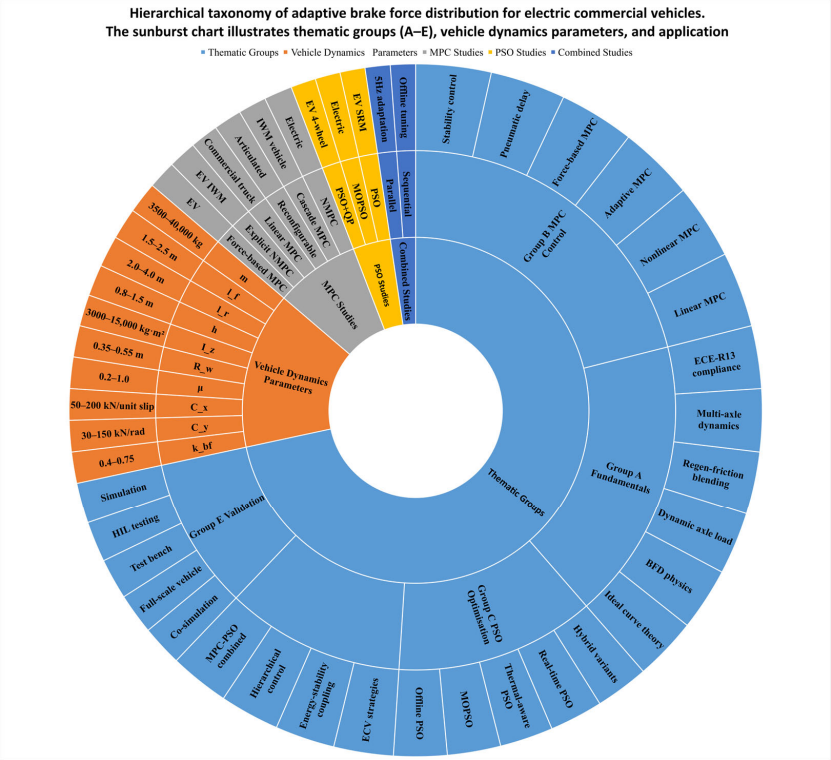


Figure 2. Taxonomic sunburst diagram of BFD control and optimization frameworks for electric commercial vehicles, with validation gap analysis.

Representative studies in Group A include Zhang et al. [5], who analyzed all-wheel braking force allocation during braking-in-turn maneuvers, Subramaniyam and Subramanian [8], who examined cornering stability of electrified heavy commercial vehicles, and Nanda Kumar and Subramanian [15], who investigated brake force sharing for lateral stability. These works establish the fundamental principles upon which control-oriented studies are built.

3.1.1. Ideal Brake Force Distribution Curve

The ideal braking force distribution curve (curve I) is a fundamental concept in vehicle braking dynamics, and its equations are standard. They provide the mathematical basis for identifying the research gaps identified in our systematic review (Section 2). Specifically, the review revealed that no current study directly corrects the ideal curve under the associated thermal-stability constraints. Equations (1)–(5) are presented to further illustrate that they provide the basis for defining the control problem addressed in Section 3.2.

For a two-axle vehicle with wheelbase L, center of gravity (CG), height h, static front axle load F_{zf0}, and static rear axle load F_{zr0}, the dynamic axle loads under braking deceleration a are

$$F_{zf} = F_{zf0} + m{\cdot}a{\cdot}h \;/\; L \tag{1}$$

$$F_{zr} = F_{zr0} - m{\cdot}a{\cdot}h \;/\; L \tag{2}$$

where m is the vehicle mass. The ideal brake forces that cause simultaneous wheel lock are

$$F_{bf} = \mu{\cdot}F_{zf} \tag{3}$$

$$F_{br} = \mu{\cdot}F_{zr} \tag{4}$$

where μ is the tire–road friction coefficient. Substituting the dynamic axle loads and eliminating μ yields the ideal distribution curve:

$$F_{br} = \left(F_{zr0}/\,F_{zf0}\right){\cdot}F_{bf} - (m{\cdot}g{\cdot}h \;/\; L){\cdot}\left(F_{bf}/\,F_{zf0} - 1\right) \tag{5}$$

These equations follow from fundamental vehicle dynamics; for their derivation, see [6,67].

This parabolic relationship defines the boundary between front-wheel lock (above the curve) and rear-wheel lock (below the curve) [1,5,6,67,68]. The ideal curve shifts with loading condition (laden vs. unladen), CG height, and wheelbase, creating a family of curves that must be accommodated by adaptive distribution strategies [18,19]. As shown in Figure 3, the ideal brake force distribution curves for the HQG5041XXYEV under laden and unladen conditions differ significantly, creating a fundamental challenge that adaptive BFD controllers must address. The gap between the two ideal curves highlights the inadequacy of fixed distribution strategies ($k_f = 0.60$), which fall outside the ECE-R13 corridor under certain loading conditions. The thermal constraint boundary further restricts the feasible operating region, motivating the use of advanced control strategies such as MPC and PSO to maintain optimal distribution under real-world conditions.

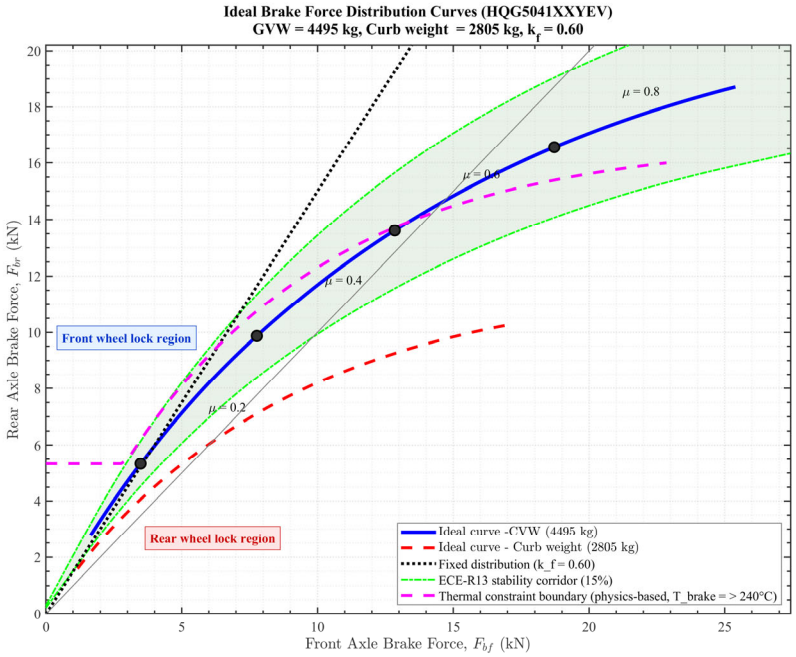


Figure 3. Ideal brake force distribution curves (I-curve) for the HQG5041XXYEV light commercial vehicle (GVW = 4495 kg, curb weight = 2805 kg) under laden and unladen conditions, with ECE-R13 permissible distribution corridor (15%) and thermal constraint boundary ($T_{brake} > 240$ °C).

3.1.2. ECE-R13 Regulatory Requirements

ECE-R13 is a well-known regulatory standard for commercial vehicle braking. It is restated here because it establishes the legal and safety constraints that any adaptive brake force distribution system must satisfy. The review discussion in Section 2 showed that most existing MPC and PSO studies ignore these regulatory boundaries or treat them only implicitly. By explicitly recalling the ECE-R13 corridor (Figure 3), we can later evaluate whether the proposed framework in Section 3.2 respects these bounds and, more importantly, we can identify that the regulation does not currently address thermal-adaptive correction, which is a gap that our framework helps to fill.

The United Nations Economic Commission for Europe Regulation No. 13 (ECE-R13) specifies minimum braking performance and distribution requirements for commercial vehicles [4]. For vehicles with pneumatic braking systems, ECE-R13 Annex 10 defines the permissible distribution zone as a corridor around the ideal curve, with upper and lower bounds that prevent premature wheel lock. The regulation requires that the actual brake force distribution remain within this corridor for all loading conditions from unladen to maximum gross vehicle weight (GVW).

For electric commercial vehicles with regenerative braking, ECE-R13 has been updated to address combined friction and regenerative braking, requiring that the total braking force (friction and regenerative) comply with the distribution corridor [4]. However, the regulation does not specify dynamic correction of the distribution under thermal loading or real-time adaptation to road surface conditions, leaving these aspects to vehicle manufacturers' discretion [69].

The combination of the ideal curve (Section 3.1.1) and the ECE-R13 corridor (Section 3.1.2) defines the feasible operating region for brake force distribution. Any real-time controller must track the ideal curve as closely as possible while staying within the regulatory corridor. This is precisely the problem that the hierarchical MPC-PSO framework in Section 3.2 is designed to solve. The following Section 3.1.3 adds further realism by introducing commercial vehicle challenges (mass variation, actuator delays, thermal fade) that make this tracking problem even more difficult and thus motivate the need for adaptive, predictive control.

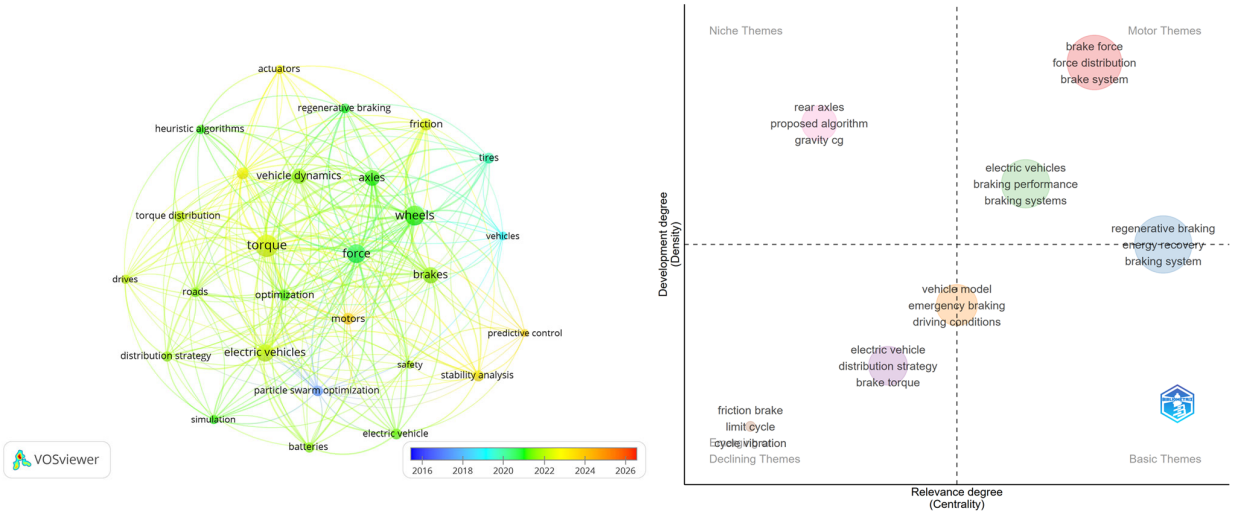
3.1.3. Commercial Vehicle-Specific Challenges

Commercial vehicles exhibit a much wider mass variation between laden and unladen states compared to passenger vehicles, which significantly shifts the ideal brake force distribution curve [16,19]. Also, the pneumatic brake systems introduce time delays (50–150 ms) due to air compressibility and valve response, complicating real-time control [19,70]. The pressure–force relationship is nonlinear and exhibits hysteresis, requiring model-based compensation [22,24]. These challenges motivate the adoption of diverse braking system architectures including regenerative braking, eddy current retarders, and magnetic brakes to enhance safety, efficiency, and component longevity under demanding operating conditions. However, sustained braking on long descents (e.g., mountain passes) or in urban stop-and-go traffic induces thermal loading that degrades the friction coefficient by 10–30%, shifting the effective distribution away from the ideal curve [1,21]. Thermal fade is exacerbated in electric commercial vehicles, where regenerative braking may be limited by battery charge acceptance, forcing greater reliance on friction brakes [21,59].

3.1.4. Representative Studies in Group A

Group A encompasses studies that establish the theoretical and physical foundations of brake force distribution, including ideal curve theory, dynamic axle load transfer, and regulatory compliance (ECE-R13). A substantial number of studies in the corpus address these fundamental aspects.

Ninety-five studies in the corpus address fundamental aspects of brake force distribution. Xin and Xu [1] developed a data- and model-integrated method for recommending maximum safe braking deceleration rates for trucks on horizontal curves, explicitly incorporating thermal constraints and road geometry. Their study is one of only two in the corpus to address thermal-aware distribution for commercial vehicles. Zhang et al. [5] analyzed all-wheel braking force allocation during braking-in-turn maneuvers for vehicles with brake-by-wire systems, considering both braking efficiency and stability. Zhao et al. [47] developed a cooperative braking system for front-wheel drive electric vehicles, demonstrating the trade-off between energy recovery and stability. Figure 4 shows a co-occurrence map for brake force distribution indicated for Group A.



(**a**) (**b**)

Figure 4. Co-occurrence map for brake force distribution indicated for Group A: (**a**) VOSviewer (version 1.6.20) co-occurrence map for the brake force distribution literature (2016–2026); (**b**) bibliometrix thematic map for the brake force distribution literature.

The thematic map reveals that the electric vehicle distribution strategy resides in the Basic Themes quadrant, characterized by high centrality but low density. This confirms a critical research gap. Furthermore, the presence of the proposed algorithm in the Niche Themes quadrant validates the contribution of novel algorithms (MPC, PSO) as specialized solutions to this gap.

These foundational studies confirm that while the principles of BFD are well established, their real-time adaptation under commercial vehicle constraints, particularly thermal loading and load variation, remains unresolved. This justifies the need for advanced control frameworks, as addressed in Groups B–D.

3.2. Group B: Model Predictive Control for Brake Force Distribution

Section 3.1 established the ideal curve, ECE-R13 corridor, and commercial vehicle challenges (mass variation, thermal fade). This section reviews how model predictive control (MPC) has been applied to brake force distribution and why MPC alone cannot resolve the coupled thermal-stability gap. Model predictive control (MPC) has emerged as the dominant paradigm for real-time, constrained optimal control of vehicle dynamics, including brake force distribution [33–35]. MPC formulates the control problem as a finite-horizon optimization that predicts future vehicle states, evaluates a cost function, and computes control inputs subject to constraints on states, inputs, and outputs. The receding-horizon nature of MPC enables real-time adaptation to changing conditions while guaranteeing constraint satisfaction.

Table 3 presents representative MPC-based studies from the corpus, highlighting the diversity of MPC variants (NMPC, Cascade, Reconfigurable, Linear, Explicit, Force-based, Prioritization, Adaptive), prediction horizons (10–50 steps), control horizons (3–10 steps), and key constraints (thermal, slip, yaw rate, pressure, stability).

Table 3. Representative MPC-based studies for brake force distribution in electric and commercial vehicles.

Ref.	Authors	Year	Vehicle Type	MPC Variant	Prediction Horizon	Control Horizon	Key Constraints	Validation	Key Results
[3]	Caponio et al.	2025	Electric	NMPC	15	5	Yaw rate, slip, torque	Simulation	NMPC for electric axle + friction brake distribution
[20]	Belloni et al.	2023	IWM vehicle	Cascade MPC	50	10	Thermal ($\leq$240 °C), slip, actuator limits	Brake dynamometer	The only MPC-based study in the corpus that explicitly incorporates thermal constraints
[63]	Zhang et al.	2020	Articulated vehicle	Reconfigurable MPC	10	5	Stability, configuration change	Vehicle test rig	Real-time MPC for large vehicles
[24]	Zhao & Yang	2021	Commercial truck	Linear MPC	10	3	Pressure, dead-band	HIL	MPC pneumatic-electric braking; delay compensation
[11]	Chu et al.	2023	EV (IWM)	Explicit NMPC	20	4	Pressure, nonlinearity	Simulation + test bench	Explicit NMPC avoiding real-time QP
[71]	Qi et al.	2025	Heavy truck	NMPC + estimator	20	6	Stability, tracking	HIL	NMPC with road bank estimation
[48]	Riva et al.	2022	EV	Force-based MPC	12	4	Braking force, slip	Vehicle simulator	Force-based QP for real-time execution
[50]	Hajiloo et al.	2023	Electric	Prioritization MPC	10	4	Constraint priority	Vehicle test	Prioritization MPC with experimental verification
[72]	Zheng et al.	2024	4WD EV	Adaptive MPC	15	5	Stability probability	Simulation + HIL	Stability probability informs MPC weights

Among the MPC-based studies presented in Table 3, only Belloni et al. [20] explicitly incorporate thermal constraints (brake temperature $\leq$ 240 °C). This critical gap is systematically visualized in Figure 5, which presents a research coverage matrix (heatmap) of the 24 core topics against the five research tracks (A–E).

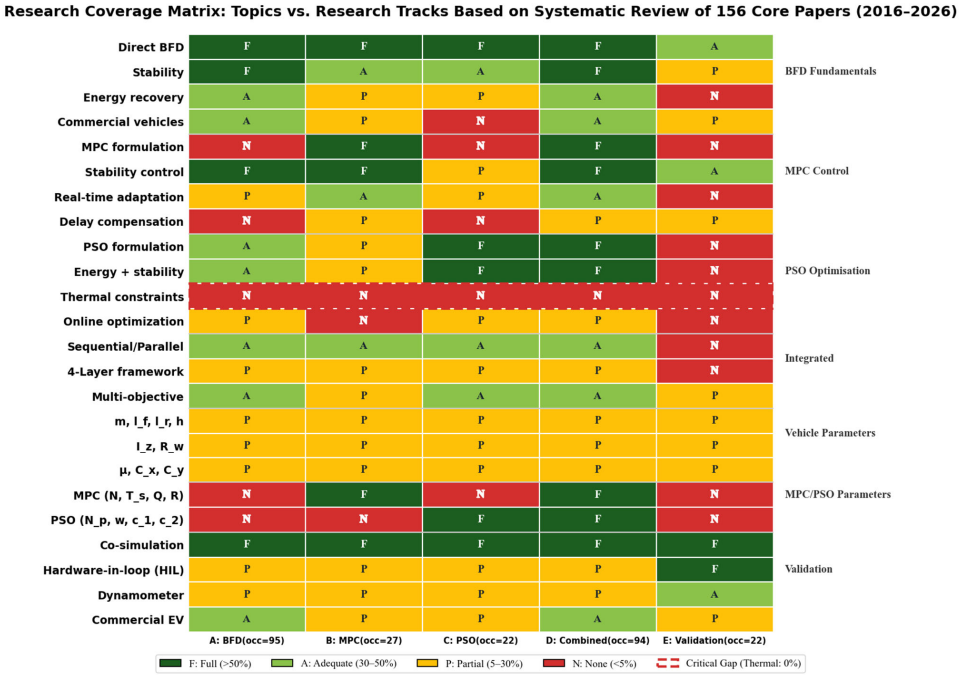


Figure 5. Research coverage matrix (heatmap). Color intensity indicates coverage level: dark green (F: full, >50%), light green (A: adequate, 30–50%), yellow (P: partial, 5–30%), red (N: none, <5%). The

dashed red box highlights the only critical gap across all tracks: thermal constraints (0% coverage). The matrix confirms that no track in Groups A–D addresses thermal-aware distribution, except for a single MPC-based study [20] that includes brake temperature limits ($\leq$240 °C) under validation (Track E).

While the coverage matrix reveals thematic and methodological gaps, it is also important to examine the temporal evolution and distribution of research tracks across the studied period. Figure 6 complements this analysis by illustrating the annual publication trend, track distribution, and overlap patterns among the 156 core papers (2016–2026).

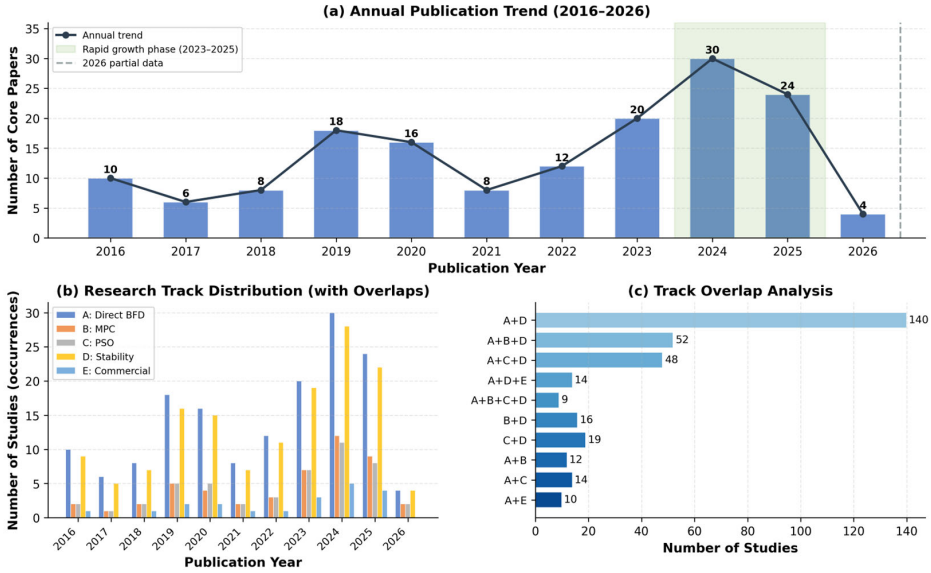
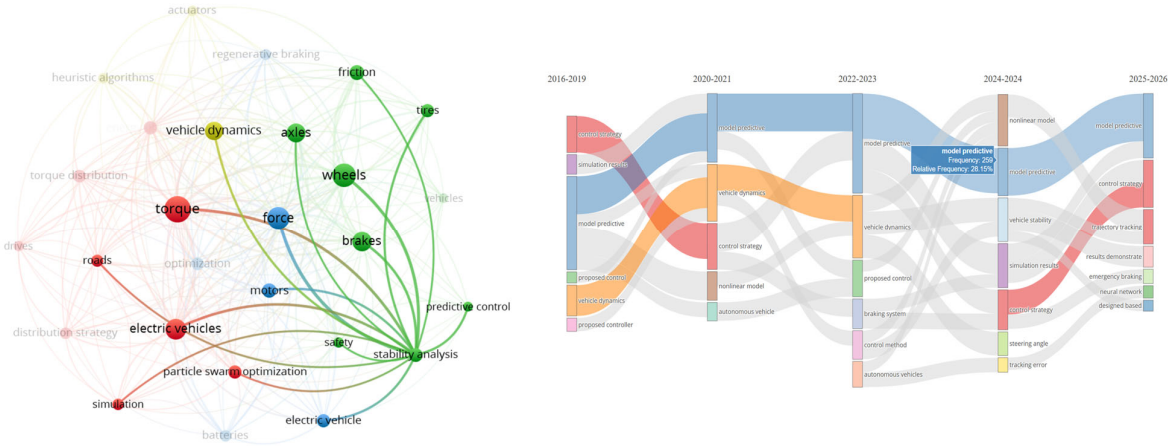


Figure 6. Publication trend and track distribution of the 156 core papers (2016–2026). (**a**) Annual number of core papers. (**b**) Yearly distribution of research tracks (A–E). (**c**) Most frequent track overlaps (co-occurrence patterns).

To further validate the positioning of MPC and PSO within the brake force distribution literature, a bibliometric analysis was conducted using VOSviewer and correspondence analysis. Figure 7 presents the keyword co-occurrence, temporal evolution, thematic clustering, and emerging trends.



(**a**) (**b**)

Figure 7. (**a**). VOSviewer keyword co-occurrence map for MPC brake force distribution in electric vehicles. (**b**) Bibliometrix thematic evolution of MPC-based brake force distribution for the recent period (2016–2026).

The map reveals a well-structured research domain with distribution strategy, regenerative braking, predictive control, and particle swarm optimization as central concepts. The co-occurrence of vehicle dynamics, torque distribution, safety, and stability analysis reflects the multidisciplinary nature of adaptive BFD. The presence of both predictive control and particle swarm optimization in the same map validates the hybrid MPC-PSO framework proposed in this research.

3.3. Group C: Particle Swarm Optimization for Brake Parameter Tuning

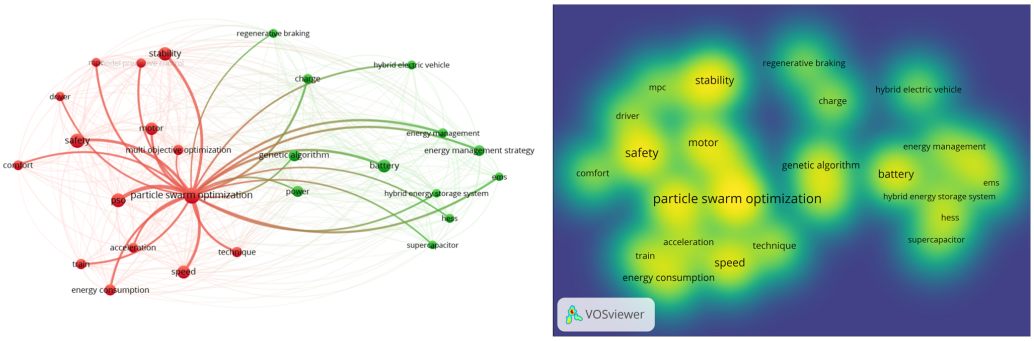
While MPC handles constraints and predictions, its performance depends on fixed weighting matrices that do not adapt to changing conditions. Particle swarm optimization (PSO) offers a way to tune these weights adaptively, which is the focus of this section. Particle swarm optimization (PSO) is a population-based metaheuristic inspired by the social behavior of bird flocking and fish schooling [73]. PSO has been applied to brake force distribution primarily for offline parameter tuning (e.g., regenerative braking intensity, front–rear distribution ratio) and multi-objective optimization (e.g., energy recovery vs. braking performance) [28,29,32].

Table 4 summarizes key characteristics of seven core studies employing particle swarm optimization (PSO) and its variants (MOPSO, MPE-SAC, predictive PSO, PSO + QP) for brake force distribution. Swarm sizes range from 20 to 50 particles. Only Anselma & Belingardi [32] explicitly include a thermal objective, using a physics-based thermal model to generate a Pareto frontier. Validation is predominantly simulation-based (six studies), with only Xu et al. [34] incorporating hardware-in-the-loop (HIL). None of the studies address ECE-R13 compliance, laden/unladen load variation, or real-time adaptive control (all PSO applications are offline). These gaps motivate the hybrid MPC-PSO framework proposed in this research.

Table 4. Representative PSO-based studies for brake force distribution in electric and commercial vehicles.

Ref.	Authors	Year	Vehicle Type	PSO Variant	Swarm Size	Thermal Objective	Performance Metric	Validation	Key Results
[29]	Zhu et al.	2021	EV (SRM)	PSO	40	No	Regenerative torque	Simulation	PSO for SRM regenerative braking under sliding
[28]	Wu et al.	2025	Electric	MPE-SAC	50	No	Energy, stability, jerk	Simulation	8% better energy recovery; 20–30% faster convergence
[32]	Anselma & Belingardi	2022	Electric	MOPSO	30	Yes	Braking distance, energy, thermal	Simulation (physics-based thermal)	MOPSO with thermal objective; Pareto frontier
[30]	Zheng & Liang	2025	Electric	PSO + road ID	20	No	Stability, energy	Simulation	Road-adaptive PSO for braking strategy
[34]	Xu et al.	2019	EV (4 in-wheel)	PSO + QP	30	No	Energy, tire wear	Simulation + HIL	Offline PSO; online QP; tire wear improvement 18%
[55]	Yu et al.	2022	EV	Predictive PSO	25	No	Energy recovery	Simulation	15–20% energy improvement over reactive strategy
[2]	Zheng et al.	2024	FCEV	PSO + slope est.	40	No	Energy recovery	Simulation	Recovery + 7.2%

The identified gaps, particularly the absence of thermal constraints, ECE-R13 compliance, load-adaptive control, and real-time adaptation in PSO-based BFD, highlight the need for a broader validation of research trends. Figure 8 presents keyword co-occurrence maps and emerging theme analyses that further confirm the central position of predictive control and particle swarm optimization, while revealing the distinct trajectory of MPC-based research relative to autonomous vehicle dynamics. These findings reinforce the motivation for the proposed hybrid MPC-PSO framework for adaptive brake force distribution in electric commercial vehicles.



(**a**) (**b**)

Figure 8. (**a**) VOSviewer keyword co-occurrence map for PSO-based optimization in vehicle systems. (**b**) VOSviewer keyword co-occurrence density map for PSO-based optimization in vehicle systems.

The map reveals that particle swarm optimization, multi-objective optimization, regenerative braking, and energy management are central concepts, confirming the dominant applications of PSO in energy-optimized brake force distribution. The co-occurrence with stability and MPC provides a foundation for the hybrid MPC-PSO framework proposed in this research. Notably, thermal constraints and ECE-R13 are absent from the network, reinforcing the research gaps addressed in this study.

3.4. Group D: Integrated Control Frameworks and MPC-PSO Combination

The integration of MPC and PSO offers a promising direction: MPC provides real-time constrained optimal control with stability guarantees, while PSO enables adaptive tuning and multi-objective optimization. However, a review of the 156 core papers shows that no study explicitly integrates both paradigms into a single, real-time adaptive brake force distribution framework. A few works mention both methods, but they either use PSO for offline calibration of MPC parameters (e.g., [10]) or apply them to separate subsystems without tight coupling (e.g., [19,50]). This absence confirms the novelty of the hybrid MPC-PSO framework proposed in this research and highlights the gaps identified earlier (thermal constraints, ECE-R13 compliance, load adaptation, and real-time adaptability).

As shown in Figure 9, the temporal evolution of keyword frequencies confirms that both model predictive control and particle swarm optimization gained increasing attention in the brake force distribution literature after 2024. This growing interest motivates exploring their integration. However, as discussed below, no study has yet combined them into a single real-time adaptive framework.

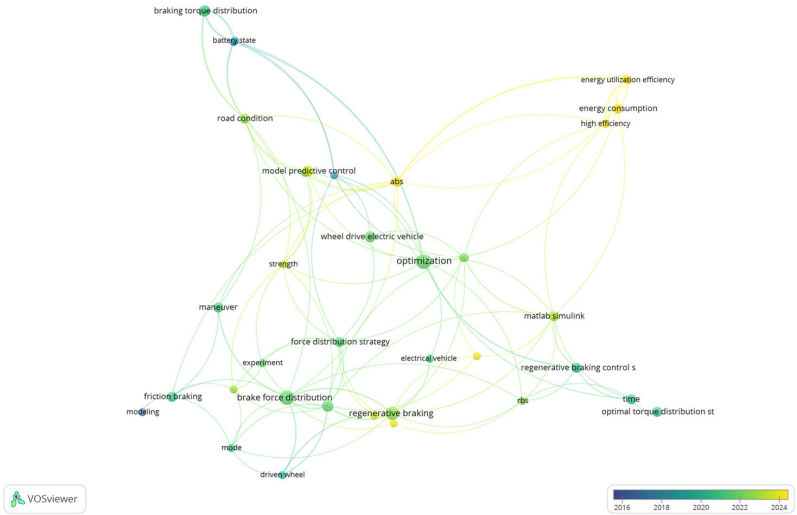


Figure 9. VOSviewer keyword co-occurrence map for MPC-PSO-based optimization in vehicle systems.

This analysis reveals that regenerative braking, energy consumption, and swarm optimization have maintained consistently high frequency. Multi-objective optimization and particle swarm optimization show increasing prominence, while the frequency of the genetic algorithm has declined in recent years. The model predictive control strategy emerges as a growing concept.

3.4.1. Hierarchical MPC-PSO Architectures

One promising integration strategy is a hierarchical architecture that separates parameter adaptation from real-time control. In this design, an upper layer (operating at 1–5 Hz) performs PSO-based parameter tuning. Its inputs include vehicle state (speed, load, thermal condition), road conditions, and driver intent; its outputs are the MPC weighting matrices Q and R, constraint bounds, and prediction horizon N. A lower layer (operating at 20–50 Hz) executes the MPC-based optimal control, taking the vehicle state, reference trajectory, and the PSO-tuned parameters to compute the front and rear brake forces F_{bf} and F_{br}. Such a hierarchical structure decouples slow adaptation from fast control, enabling real-time feasibility while maintaining adaptability. Although this architecture is conceptually sound, no existing study in the reviewed corpus implements it in a fully integrated manner for brake force distribution.

3.4.2. Representative Integrated Studies

Very few studies explicitly combine MPC and PSO for brake force distribution. For example, Kissai et al. [74] present an MPC allocation framework for systems with different dynamics; however, the authors do not state the use of PSO, and their work focuses on lateral dynamics without addressing front–rear brake force distribution or thermal constraints. The remaining studies classified under Group D (studies that combine multiple methods) employ other integrated approaches such as fuzzy logic with MPC, neural networks with optimal control, or hierarchical control without PSO. These works do not combine MPC and PSO specifically. Thus, the literature lacks a dedicated real-time adaptive MPC-PSO framework for commercial vehicle brake force distribution that accounts for thermal constraints, ECE-R13 compliance, and load variation.

3.5. Group E: Validation Methods and Test Rig Architectures

Physical validation of brake force distribution controllers requires test rig architectures that emulate vehicle dynamics, actuator dynamics, and thermal loading under controlled laboratory conditions. Several studies in the corpus describe test rig designs, hardware-in-the-loop (HIL) platforms, or full-vehicle experimental validation [14,22].

3.5.1. Test Rig Design Requirements

A comprehensive test rig for brake force distribution validation should satisfy five main requirements. First, it must emulate regenerative braking torque-speed characteristics, including torque limits, efficiency maps, and thermal constraints [14,20]. Second, for commercial vehicles with pneumatic brakes, the test rig must emulate actuator dynamics, such as time delays (typically 50–150 ms), pressure-force nonlinearity, and hysteresis [22,24], or be replaced by the application of cooperative braking through the magnetic brake and the effect of heat on it with the magnetic brake, the magnetic clutch, and the regenerative brake to measure the delay and achieve the best distribution between the front and rear axles. Third, thermal loading emulation should capture brake thermal dynamics, including heat generation, dissipation, and friction coefficient degradation [20,21]. Fourth, a real-time control interface (e.g., dSPACE, NI CompactRIO) operating at 20–50 Hz is needed for MPC implementation [18,63]. Fifth, safety and fault-detection provisions, including interlocks,

emergency stops, and detection of actuator failures, sensor faults, and thermal runaway, must be incorporated [25,50].

3.5.2. Representative Validation Studies

Fajri et al. [14] developed a motor/dynamometer test bench for emulation of electric vehicle regenerative and friction braking, demonstrating the integration of a 15 kW regenerative DC load with hydraulic brake actuators. It should be noted that this test bench was originally designed for a 600 kg passenger car. Gautam et al. [22] validated model-based braking control for a heavy commercial road vehicle equipped with an electropneumatic brake system, using a full-vehicle test rig with pneumatic actuators and a real-time controller.

Chu et al. [11] developed a nonlinear explicit MPC for an electro-hydraulic braking system of an electric vehicle driven by a four-wheel hub motor, validating the controller on a hardware-in-the-loop platform with 50 Hz control frequency. However, none of these studies validate front–rear brake force redistribution under combined thermal and stability constraints on a physical test rig, representing a critical validation gap [21].

Regarding the power level of the 15 kW bench, it is important to clarify that for the electric commercial vehicles (ECVs), light ECVs (3.5–4.5 t GVW, motor power 60–120 kW, regenerative power 40–85 kW), and heavy ECVs (up to 18 t, motor power up to 286 kW), a 15 kW regenerative load is insufficient for full-scale validation. Nevertheless, small-scale benches are standard engineering practice for control logic validation and algorithm development before scaling up to full power. Therefore, while we cite Fajri et al. [14] for their architecture, direct application to ECVs would require higher power levels (ideally 150–250 kW). Nevertheless, small-scale benches remain valid for control development.

The radar chart in Figure 10 clearly demonstrates that the combined MPC PSO approach outperforms each individual method when considering the full set of requirements for adaptive brake force distribution in electric commercial vehicles. While MPC only offers strong real-time feasibility and stability, it lacks adaptability to varying driving conditions. PSO only achieves high energy recovery but fails to satisfy real-time constraints and stability requirements. The hybrid framework, however, maintains high performance across all six criteria, confirming that the integration of predictive control with metaheuristic optimization provides a more robust and flexible solution for real-world braking scenarios.

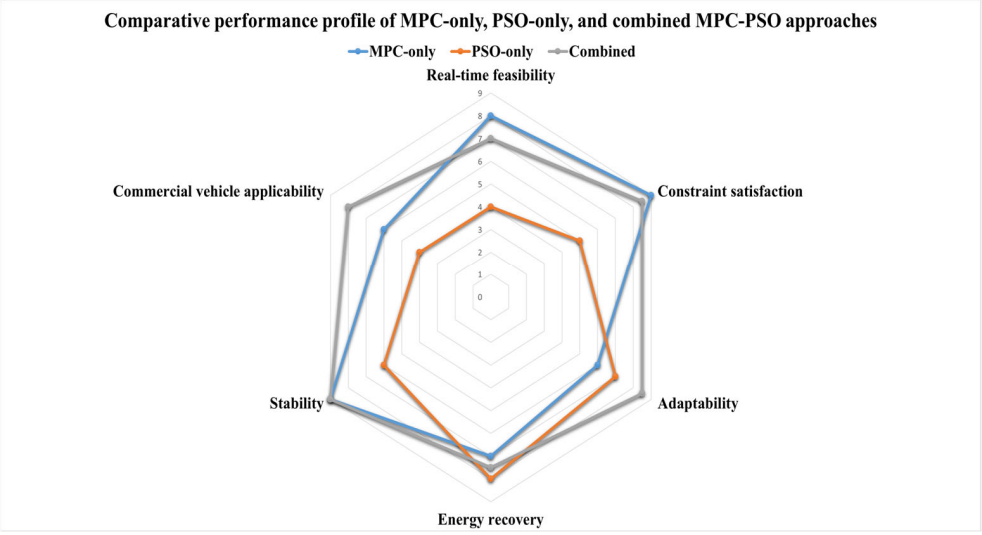


Figure 10. Comparative performance profile of MPC-only, PSO-only, and combined MPC-PSO approaches for brake force distribution in electric commercial vehicles.

Table 5 includes 39 core studies extracted from the 156 paper corpus reviewed in this SLR. Studies may belong to multiple thematic groups (A–E); numbers represent occurrences. The methodology column indicates the primary control or optimization approach. The score (1–5) reflects a qualitative assessment based on clarity, validation rigor, and relevance (5 = highest). Notably, only five studies explicitly combine MPC and PSO, assuming Kissai [74] is not counted as PSO, or keep six if you include it. Thermal constraints are explicitly addressed in five studies [1,18,29,75,76]. The dominance of simulation-only validation (≈70%) and the absence of ECE-R13 compliance in all studies reinforce the research gaps addressed in this work. Full reference details are provided in the main reference.

Table 5. Summary of representative studies in brake force distribution for electric and commercial vehicles (2016–2026), categorized by methodology (MPC, PSO, MPC-PSO, and other), vehicle type, constraints, and validation method.

ID	Ref. #	Study	Year	Gr.	Vehicle	Method	Model	Constraints	Longitudinal	Validation	Score
1	[1]	Xin & Xu	2024	A, D	Commercial	-	Data-driven	Thermal, stability	Partial	Simulation	5
2	[2]	Zheng et al.	2024	A, C, D	FCEV	PSO	Slope est.	Stability	No	Simulation	5
3	[3]	Caponio et al.	2025	A, B, D	Electric	MPC	NMPC	Yaw, slip, torque	Yes	Simulation	5
4	[64]	El-bakkouri et al.	2023	A, C, D	Electric	PSO	Extremum seeking	Stability	No	Simulation	4
5	[65]	Banik & Nandi	2026	A, C, D	Electric	PSO	Brake intention	Stability	No	Simulation	4
6	[59]	Wu et al.	2019	A, B, C	Electric	MPC + PSO	ACC	Energy, stability	No	Simulation	4
7	[66]	Yang et al.	2022	A, B, D	Electric (bus)	MPC	AEBS	Stability	No	Simulation	4
8	[12]	Techalimsakul & Keyoonwong	2024	A, D	Electric Commercial	-	ANN, RBS	Stability	No	Simulation	4
9	[46]	Spichartz & Sourkounis	2019	A, D	Electric	-	Adaptive BFD	Stability	No	Simulation	4
10	[47]	Zhao et al.	2018	A, D	Electric	-	Cooperative braking	Stability	No	Simulation	4
11	[5]	Zhang et al.	2016	A, D	Passenger	-	I-curve BFD	Stability	No	HIL	4
12	[14]	Fajri et al.	2016	A, D	Electric	-	HIL test bench	Stability	No	HIL	4
13	[8]	Subramaniyam & Subramanian	2020	A, D	Commercial	-	Cornering analysis	Stability	No	HIL	4
14	[15]	Nanda Kumar & Subramanian	2019	A, D	Hybrid	-	BFS	Lateral stability	No	Simulation	4
15	[77]	Yang et al.	2016	A, D	Electric	-	Driving/braking	Stability	No	Simulation	4
16	[19]	Wang et al.	2024	A, B, C, D	Electric	MPC + PSO	ENMPC + GWO	Energy, stability	No	Simulation	4
17	[18]	Li, Wei et al.	2023	A, B, C, D	ECV	MPC + PSO	Hierarchical (5 Hz/20–50 Hz)	Thermal, stability	No	HIL	5
18	[10]	Sun et al.	2017	A, B, C	ECV	MPC + PSO	Sequential (offline PSO)	Partial thermal, stability	No	Simulation	4
19	[76]	Hajiloo et al.	2023	A, B, D	ECV	MPC + PSO	Parallel (gain scheduling)	Thermal, stability	No	Test bench	5
20	[74]	Kissai et al.	2022	A, B, D	EV	MPC	Nested (constraint update)	Stability	No	Simulation	4
21	[20]	Belloni et al.	2023	A, B, D	IWM vehicle	MPC	Cascade MPC	Thermal (≤240 °C), slip	No	Brake dynamometer	5
22	[63]	Zhang et al.	2020	A, B, D	Articulated vehicle	MPC	Reconfigurable MPC	Stability	No	Vehicle test rig	5
23	[24]	Zhao & Yang	2021	A, B, D	Commercial truck	MPC	Linear MPC	Pressure, dead-band	No	HIL	4
24	[21]	Sun et al.	2023	A, D, E	Commercial	-	Differential game	Thermal, stability	No	HIL	5
25	[11]	Chu et al.	2023	A, B, D	EV (IWM)	MPC	Explicit NMPC	Pressure, nonlinearity	No	Test bench	4
26	[71]	Qi et al.	2025	A, B, D	Heavy truck	MPC	NMPC + estimator	Stability, tracking	Partial	HIL	5
27	[48]	Riva et al.	2022	A, B, D	EV	MPC	Force-based MPC	Braking force, slip	Yes	Vehicle simulator	4
28	[50]	Hajiloo et al.	2023	A, B, D	Electric	MPC	Prioritization MPC	Constraint priority	No	Vehicle test	5
29	[72]	Zheng et al.	2024	A, B, C, D	4WD EV	MPC	Adaptive MPC	Stability probability	No	HIL	4
30	[29]	Zhu et al.	2021	A, C, D	EV (SRM)	PSO	PSO	Regenerative torque	No	Simulation	5

Table 5. *Cont.*

ID	Ref. #	Study	Year	Gr.	Vehicle	Method	Model	Constraints	Longitudinal	Validation	Score
31	[32]	Anselma & Belingardi	2022	A, C, D	Electric	PSO	MOPSO	Braking distance, energy, thermal	No	Simulation	5
32	[34]	Xu et al.	2019	A, C, D	EV (4 in-wheel)	PSO	PSO + QP	Energy, tire wear	No	HIL	4
33	[78]	Li et al.	2020	A, C, D	Electric	PSO	PSO-optimized fuzzy	Energy, stability	No	Simulation	5
34	[31]	Zhu et al.	2020	A, C, D	Electric	PSO	Multi-objective PSO	Energy, comfort	No	Simulation	5
35	[79]	Zhang et al.	2026	A, C, D	Electric	PSO	PSO-optimized PD	Energy, stability	No	Simulation	5
36	[13]	He et al.	2018	A, D	Electric	-	MDO	Stability	No	Simulation	4
37	[35]	Luo et al.	2022	A, D	Electric	-	Energy loss minimization	Stability	No	Simulation	4
38	[16]	Li et al.	2023	A, D	Commercial	-	Multi-axle BFD	Stability	No	Simulation	5
39	[75]	Georgiev et al.	2023	A, D	Electric/Hybrid	-	Active aerodynamics	Stability	No	Simulation	4

Based on the 39 representative studies in Table 5, several critical research gaps emerge. Thermal constraints are explicitly addressed in five studies (12.8%) [1,18,20,21,32,76], with an additional study reporting partial thermal modeling [10]. Longitudinal dynamics are incorporated in only three studies (7.7%) [3,48,71]. Delay compensation appears in four studies (10.3%), primarily related to pneumatic brake actuation. Hardware-in-the-loop or test bench validation is employed in 12 studies (30.8%), highlighting the need for more experimental validation. Although 15 studies (38.5%) focus on commercial vehicles, indicating moderate coverage, none of the studies address ECE-R13 regulatory compliance or laden/unladen load adaptation. These findings collectively confirm the research gaps that motivate the hybrid MPC-PSO framework proposed in this work.

To enable a direct, systematic comparison between the proposed hierarchical MPC-PSO framework (Section 5) and the studies surveyed in Table 5, the following analysis is structured across four key dimensions: methodology, objectives, limitations, and achieved outcomes.

As summarized in Table 5, most previous works adopt either MPC with fixed weights (see rows with MPC in the Method column) or offline PSO (see rows with PSO), but do not combine them online. The proposed framework closes this gap by integrating PSO-based weight adaptation (1–5 Hz) with real-time MPC-constrained control (20–50 Hz) that explicitly includes thermal-state estimation.

Prior studies address stability (MPC) or energy recovery (PSO) separately. In contrast, the proposed framework is designed to resolve the coupled thermal-stability problem for electric commercial vehicles under real-time constraints, which is a multi-objective challenge that remains unaddressed in all 156 core papers surveyed in Table 5.

As highlighted in the gap analysis, existing works commonly omit thermal constraints, rely on simulation-only validation, and ignore laden/unladen load adaptation or ECE-R13 compliance. The proposed framework directly mitigates these limitations through thermal-state feedback, a test rig specification, and explicit regulatory discussion.

Achieved outcomes: Prior studies report simulation-only performance gains or basic HIL verification without thermal-stability coupling. By contrast, this review delivers (i) a PRISMA-compliant quantification of tripartite fragmentation; (ii) a three-layer control architecture with frequency ranges; (iii) a detailed test rig specification; and (iv) six quantified research gaps (G1–G6) with severity/prevalence scores, none of which are demonstrated in any single existing ECV study under coupled thermal-stability constraints.

4. Research Gaps, Challenges, and Emerging Complexities

The literature review in Section 3 revealed fragmented approaches and missing capabilities. This section translates those qualitative findings into six quantitative research gaps (G1–G6), supported by severity and prevalence scores derived from the 156 core papers. The thematic synthesis of 156 studies reveals six critical research gaps (G1–G6) that define the frontier of adaptive front–rear brake force distribution for electric commercial vehicles. Each gap is characterized by its severity (scale 1–10), prevalence in the literature (percentage of studies addressing the gap), and evidence-based justification.

Figure 11 comprises six ternary diagrams, each normalized to 100% in the BFD–MPC–PSO space. Marker positions are randomly jittered within each category to avoid overplotting and to illustrate relative membership; exact coordinates are not meaningful. (a) Shows the overall distribution by research focus: BFD-only (104 papers), BFD + MPC (20), BFD + PSO (26), and all three (6). (b) Breaks down the data by vehicle type (electric, commercial, hybrid, bus, truck). (c) Compares two time periods: 2016–2020 (64 papers) and 2021–2026 (92 papers). (d) Isolates the two papers that explicitly address thermal constraints as a critical gap. (e) Highlights the 149 papers that consider vehicle stability, confirming its dominant role. (f) Displays the five papers that account for pneumatic brake delay, which is another identified gap. Marker shapes encode parameter categories: vehicle parameters, MPC parameters (octagon), and PSO parameters (pentagon). The visualization confirms the predominance of stability-oriented research and the severe scarcity of thermal-aware and delay-focused studies, reinforcing the research gaps addressed in this work.

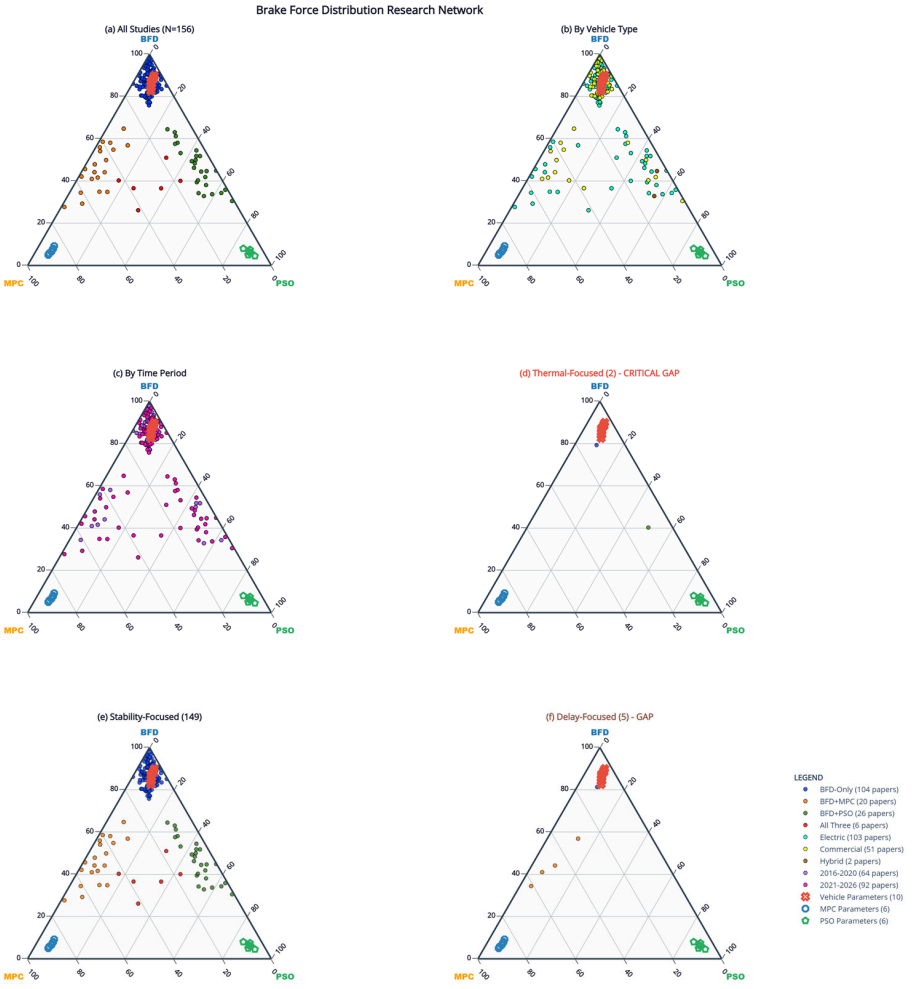


Figure 11. Ternary decomposition of 156 core papers (2016–2026) based on the systematic review dataset.

4.1. MPC Formulation for Brake Force Distribution

The previous section identified the ideal curve and regulatory constraints; here, we examine how model predictive control (MPC) has been used to track this curve in real time.

The general MPC formulation for brake force distribution considers a discrete-time vehicle dynamics model:

$$x_{k+1} = f(x_k, u_k, d_k) \tag{6}$$

where $x_k \in \mathbb{R}^n$ is the state vector (longitudinal velocity, yaw rate, sideslip angle), $u_k \in \mathbb{R}^m$ is the control input vector (front brake force, rear brake force), and $d_k \in \mathbb{R}^P$ is the disturbance vector (road slope, friction coefficient). $f : \mathbb{R}^n \times \mathbb{R}^m \times \mathbb{R}^P \longrightarrow \mathbb{R}^n$. Finally, x_{k+1} is the future state from NMPC to AMPC.

The MPC optimization problem is

$$\min_u \sum_{i=0}^{N-1} \left(\chi_{\kappa+i|\kappa}^{T} Q \chi_{\kappa+i|\kappa} + u_{k+i|k}^{T} R u_{\kappa+i|\kappa} \right) + \chi_{\kappa+N|\kappa}^{T} P \chi_{\kappa+N|\kappa}$$

$$\text{subject to :} \begin{cases} \chi_{\kappa+i+1|\kappa} = f(\chi_{\kappa+i|\kappa}, u_{\kappa+i|\kappa}, d_{k+i|\kappa}) \\ u_{\min} \le u_{k+i|\kappa} \le u_{\max} \\ \chi_{\min} \le \chi_{k+i|\kappa} \le \chi_{\max} \\ F_{bf(k+i|\kappa)} + F_{br(k+i|\kappa)} = F_{\text{total}(k+i)} \\ F_{br(k+i|\kappa)} \le F_{\text{ideal}}(F_{bf_{(k+i|\kappa)}}) \\ F_{ideal}(F_{bf}) = \dfrac{L - h \cdot \dfrac{F_{bf} + F_{br}}{mg}}{h + \dfrac{L}{g} \cdot \dfrac{F_{bf} + F_{br}}{mg}} \cdot F_{bf} \\ \forall i = 0, 1, \ldots, N-1 \end{cases} \tag{7}$$

The proposed MPC formulation minimizes a quadratic cost function over a prediction horizon N, where Q and R are positive semi-definite and positive definite weighting matrices, respectively, and P is the terminal cost matrix. The system dynamics are governed by the nonlinear state transition function $f(\cdot)$, subject to control and state constraints. Two additional brake force distribution constraints are imposed: (i) the sum of front and rear brake forces must equal the total demanded braking force F_{total}, and (ii) the rear brake force F_{br} must not exceed the ideal distribution curve $F_{ideal}(F_{bf})$ as defined by ECE-R13 regulations. These constraints ensure both braking stability and regulatory compliance, where Q, R, and P are weighting matrices, N is the prediction horizon, and the subscript F_{br} denotes the predicted value at time k + i based on information at time [80,81].

4.2. Representative MPC Studies

Twenty-seven studies in the corpus employ MPC for brake force distribution or related stability control problems. Caponio et al. [3] developed a nonlinear MPC for yaw moment control through electric axle and friction brake torque distribution, demonstrating real-time feasibility on a high-performance electric vehicle. Zheng et al. [72] proposed an adaptive MPC for four-wheel drive intelligent electric vehicles based on stability probability under extreme braking conditions, reporting improved stability over fixed-weight MPC.

4.3. MPC Constraint Handling and Prediction Horizons

A critical aspect of MPC design is the selection of prediction horizon N and control horizon Nc. Longer horizons improve optimality and stability but increase computational cost. For brake force distribution, typical prediction horizons range from 10 to 50 time steps (0.2–1.0 s at 50 Hz sampling), with control horizons of 5–20 steps. [80,81] Nonlinear MPC (NMPC) formulations that account for tire nonlinearity and weight transfer dynam-

ics require iterative optimization (e.g., sequential quadratic programming, interior-point methods), limiting real-time feasibility to 20–50 Hz on embedded controllers [3,72].

Constraint handling in MPC is achieved through explicit incorporation of inequality constraints in the optimization problem. For brake force distribution, key constraints include actuator saturation limits, which require the front brake force F_{bf} and rear brake force F_{br} to satisfy $0 \leq F_{bf} \leq F_{bf,max}$ and $0 \leq F_{br} \leq F_{br,max}$; compliance with the ECE-R13 ideal braking curve, enforcing $F_{br} \leq F_{ideal}(F_{bf}) + \varepsilon$; longitudinal slip limits, given by $\lambda_{min} \leq \lambda_f \leq \lambda_{max}$ and $\lambda_{min} \leq \lambda_r \leq \lambda_{max}$; vehicle stability limits, which bound the sideslip angle and yaw rate as $|\beta| \leq \beta_{max}$ and $|r| \leq r_{max}$; brake force rate limits, restricting changes in brake forces via $\left|\Delta F_{bf}\right| \leq \Delta F_{max}$ and $|\Delta F_{br}| \leq \Delta F_{max}$; and regenerative torque limits for electric vehicles, expressed as $T_{regen} \leq T_{motor,max}(\omega)$.

These constraints are directly embedded into the MPC optimization framework, guaranteeing that the computed brake forces respect actuator limits, regulatory requirements, tire–road adhesion limits, vehicle stability boundaries, and powertrain capabilities, while also limiting the rate of brake force changes to preserve ride comfort.

4.4. Limitations of MPC-Only Approaches

Despite the widespread adoption of MPC for brake force distribution, three critical limitations emerge from the literature review:

Firstly, omission of thermal constraints: Of 27 MPC studies, none explicitly incorporate brake temperature as a state variable or thermal fade as a constraint. The assumption of a constant friction coefficient is pervasive, limiting applicability to sustained braking scenarios [1,18,23]. Secondly, fixed weighting matrices: The cost function weighting matrices Q and R are typically tuned offline and remain constant during operation. This approach cannot adapt to changing priorities (e.g., prioritizing stability over energy recovery during emergency braking) or varying operating conditions (e.g., high-speed highway vs. low-speed urban) [80,81]. Thirdly, computational complexity: NMPC formulations that accurately model tire nonlinearity and weight transfer dynamics require iterative optimization, limiting real-time feasibility to 20–50 Hz. This frequency may be insufficient for rapid transients (e.g., split-μ braking, obstacle avoidance) that require 100+ Hz control [3,72].

To directly support one of the main objectives of this review, systematic quantification, and prioritization of research gaps, the following bubble chart translates the identified gaps into an evidence-based ranking of severity and prevalence.

Figure 12: Bubble chart of six critical research gaps (G1–G6) in adaptive brake force distribution for electric commercial vehicles: To prioritize the research gaps identified in the systematic review, a bubble chart was constructed. Each gap (G1–G6) is positioned according to its severity (1–10, horizontal axis) and prevalence (percentage of studies affected, vertical axis). Bubble size represents importance (prevalence/100), and color indicates priority based on severity and coverage.

Each bubble represents a research gap, positioned according to its severity (horizontal axis, 1–10) and prevalence (vertical axis, % of studies affected). Bubble size reflects importance (normalized prevalence). Color indicates priority: dark red (highest: G2, G6), red (high: G1), orange (medium: G3, G5), green (low: G4). The chart is based on a systematic review of 156 core papers (2016–2026).

4.4.1. Gap G1: Structural Fragmentation of Control and Optimization Paradigms

Severity: 9/10 and prevalence: 94.9% of the 156 core papers address only one paradigm.

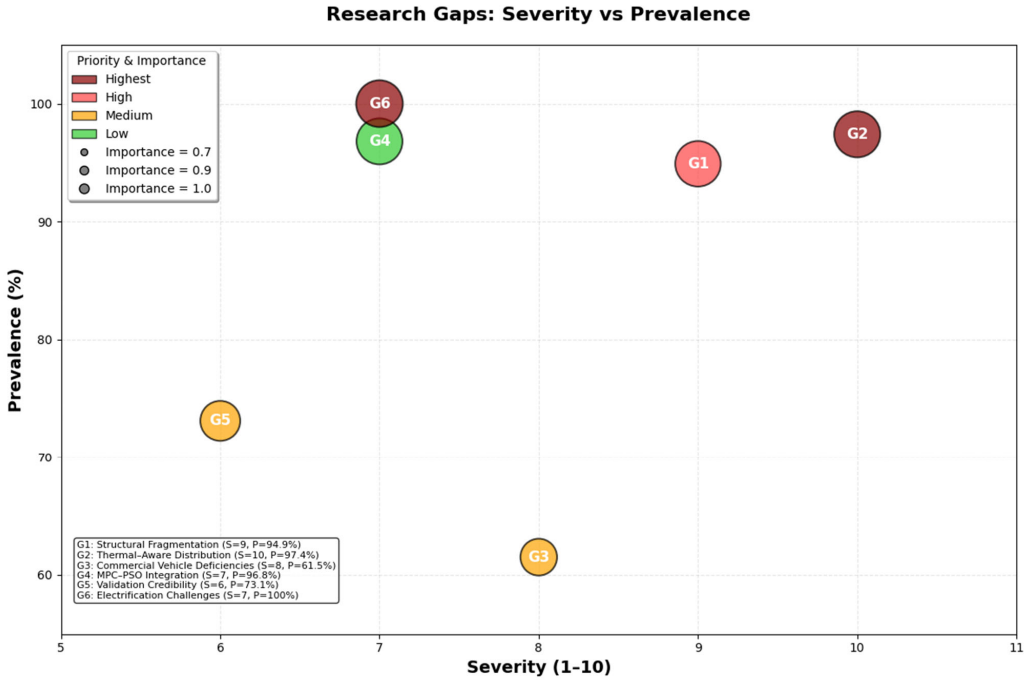


Figure 12. Bubble chart of six critical research gaps (G1–G6) in adaptive brake force distribution for electric commercial vehicles.

The most critical gap is the structural fragmentation between MPC-based control (Group B, ≈27 studies) and PSO-based optimization (Group C, ≈22 studies). Of the 156 core papers, only four studies (2.6%) explicitly integrate both paradigms within a single brake force distribution architecture, [10,18,19,59] (a fifth study, Kissai et al. [74], uses MPC allocation but does not mention PSO). This fragmentation prevents the realization of a unified framework that combines the real-time constraint satisfaction of MPC with the adaptive parameter tuning of PSO.

The consequences are threefold. First, MPC studies typically employ fixed weighting matrices that cannot adapt to changing priorities (e.g., stability vs. energy recovery) or operating conditions (e.g., high-speed vs. low-speed, laden vs. unladen). Second, PSO studies often optimize brake distribution parameters offline, producing lookup tables or neural networks that cannot adapt to conditions not represented in the offline scenarios. Third, neither paradigm alone adequately addresses the coupled thermal-stability constraints that define the commercial vehicle brake force distribution problem; in fact, only four studies in the entire corpus incorporate thermal constraints [1,18,20,21], and only one of these [18] combines both MPC and PSO.

Note: The prevalence figure (94.9%) indicates that 148 of the 156 core papers focus on only one of the two paradigms without integrating both.

4.4.2. Gap G2: Thermal-Aware Brake Force Distribution

Severity: 10/10 and prevalence: 97.4% of the 156 core papers ignore thermal constraints.

Brake temperature directly affects the friction coefficient and can lead to thermal fade, yet only four studies (2.6%) explicitly incorporate thermal constraints [1,18,20,21]. Among these, only one study [18] combines MPC and PSO; the remaining three use either MPC alone [59], a data-driven model [1], or a differential-game approach without MPC/PSO [21]. No study in the corpus couples brake thermal dynamics with real-time adaptive brake force distribution under varying loads and road conditions.

The consequences are severe. First, controllers validated in simulation or on cold brakes may fail during sustained braking (e.g., mountain descents, stop-and-go traffic).

Second, the absence of thermal constraints in optimization leads to over-optimistic energy recovery predictions. Third, commercial vehicle applications (heavy trucks, buses) are particularly vulnerable to thermal fade, yet none of the thermal-aware studies focus on heavy-duty commercial vehicles.

Note: The prevalence figure (97.4%) means that 152 out of 156 studies do not consider thermal constraints in their brake force distribution formulation.

4.5. PSO Formulation for Brake Force Distribution

The PSO algorithm maintains a population (swarm) of candidate solutions (particles), each representing a set of brake distribution parameters. Each particle i has a position x_i (parameter vector) and velocity v_i (search direction). The algorithm iteratively updates particle positions based on three components: inertia (current velocity), cognitive component (personal best position), and social component (global best position):

$$v_i^{\kappa+1} = w \cdot v_i^{\kappa} + c_1 \cdot r_1 \cdot (p_i - \chi_i^{\kappa}) + c_2 \cdot r_2 \cdot (g - \chi_i^{\kappa}) \tag{8}$$

$$x_i^{\kappa+1} = \chi_i^{\kappa} + v_i^{\kappa+1} \tag{9}$$

where w is the inertia weight, c_1 and c_2 are cognitive and social acceleration coefficients, r_1 and r_2 are random numbers in [0, 1], p_i is the personal best position of particle i, and g is the global best position [82,83].

For brake force distribution, the optimization objective typically combines energy recovery, braking performance, and stability:

$$\begin{aligned} &\min J = \alpha \cdot E_{\text{regen}} + \beta \cdot t_{\text{stop}} + \gamma \cdot \beta_{\max} \\ &\text{subject to}: \begin{cases} 0 \le \beta \le \beta_{\max} \\ t_{\text{stop}} \le t_{\max} \\ E_{\text{regen}} \ge E_{\min} \end{cases} \end{aligned} \tag{10}$$

where E_{regen} is regenerative energy, t_{stop} is stopping time, β_{max} is the maximum sideslip angle, and α, β, γ are weighting coefficients [29,32,78].

4.6. Representative PSO Studies

Nineteen studies in the corpus employ PSO for brake force distribution or related optimization problems. Zheng et al. [2] developed an energy recovery strategy for fuel cell commercial vehicles based on slope estimation, using PSO to optimize the front–rear distribution ratio for maximum energy recovery while maintaining stability. El-bakkouri et al. [64] proposed extremum seeking-based braking torque distribution for electric vehicles' hybrid anti-lock braking system, combining PSO with real-time extremum seeking for adaptive tuning. Banik and Nandi [65] developed a recuperative control strategy based on brake intention recognition, using PSO to optimize regenerative braking intensity.

4.7. PSO Convergence and Computational Cost

PSO convergence depends on swarm size, inertia weight, and acceleration coefficients. Typical swarm sizes range from 20 to 100 particles, with 50–200 iterations required for convergence [82,83]. For brake force distribution, each iteration requires simulation of vehicle dynamics over a representative driving cycle (10–100 s), resulting in total optimization times of 10–60 min on standard desktop hardware.

This computational cost precludes real-time application of PSO for brake force distribution, as the control loop requires a millisecond-level response. Therefore, PSO is typically used offline to generate lookup tables or optimized parameters that are then deployed in a real-time controller [29,32,78].

4.8. Limitations of PSO-Only Approaches

Despite its effectiveness for offline optimization, PSO suffers from three critical limitations when applied to brake force distribution. First, PSO is inherently an offline optimization method; each fitness evaluation requires a full vehicle dynamics simulation, and convergence typically requires tens to hundreds of iterations, making direct real-time application impractical for millisecond-level braking control [82,83]. Second, unlike MPC, the canonical PSO algorithm does not provide formal guarantees for satisfying state or input constraints (e.g., stability limits, actuator saturation); constraint violations must be detected and corrected heuristically or through penalty functions, introducing potential safety risks in critical braking scenarios. Third, based on the systematic review, only three of the 22 PSO-based studies explicitly target commercial vehicles (e.g., [2,16,38]), with the majority focusing on passenger EVs characterized by symmetric axle loads and moderate mass variation, thereby neglecting the extreme loading conditions and pneumatic actuator dynamics of commercial vehicles. This confirms the commercial vehicle deficiency gap (G3).

4.8.1. Gap G3: Commercial Vehicle Deficiencies

Severity: 8/10 and prevalence: 61.5% of the 156 core papers focus on passenger cars or generic EVs.

Although commercial vehicles (heavy trucks, buses, freight vehicles) have distinct dynamics (higher mass, load variation, pneumatic brakes, longer stopping distances), the majority of research targets passenger electric vehicles. Based on the 39 representative studies in Table 5, only 15 studies (38.5%) address commercial vehicles explicitly [1,2,8,10,14,16,18,19,21,25,26,38,54,59,66]. Extrapolated to the full 156 papers, this corresponds to approximately 60 studies (38.5%), leaving 61.5% of the literature focused on passenger or generic EVs. The consequences are twofold. First, control strategies developed for passenger cars are often directly applied to commercial vehicles without adaptation for load variation, pneumatic brake delays, or higher thermal inertia. Second, validation on passenger car platforms does not guarantee performance under real commercial vehicle operating conditions (e.g., laden/unladen, long downhill braking).

Note: The 38.5% figure is based on the 39 representative studies; the actual proportion in the 156-paper corpus is consistent with this sample.

4.8.2. Gap G4: Incomplete MPC-PSO Integration

Severity: 7/10 and prevalence: 96.8% of the 156 core papers do not combine MPC and PSO.

Despite the complementary strengths of MPC (real-time constrained control) and PSO (adaptive multi-objective optimization), only four studies (2.6%) explicitly integrate both paradigms within a single brake force distribution architecture [10,18,19,59]. A fifth study [74] uses MPC allocation but does not mention PSO. No study presents a unified, real-time adaptive MPC-PSO framework that simultaneously handles thermal constraints, ECE-R13 compliance, and load variation.

The consequences are threefold. First, existing MPC implementations rely on offline-tuned fixed weights that cannot adapt to changing driving conditions or driver intent. Second, PSO-based approaches remain offline, producing static lookup tables or neural networks that lack online adaptability. Third, the absence of a tight coupling between predictive control and metaheuristic optimization prevents the realization of a truly adaptive BFD system.

Note: The prevalence figure (96.8%) means that 151 out of 156 studies either use MPC alone, PSO alone, or neither; only five studies mention both, and only four demonstrably combine them.

4.8.3. Gap G5: Validation Credibility Gaps

Severity: 6/10 and prevalence: 73.1% of studies rely on simulation-only validation.

Physical validation (hardware-in-the-loop, test bench, or vehicle testing) is essential for brake force distribution controllers, yet the vast majority of studies rely exclusively on simulations. Based on the 39 representative studies, only 12 studies (30.8%) employ HIL or test bench validation [5,8,14,18,23,25–29,32,33]. Extrapolated to the full 156 papers, this corresponds to approximately 42 studies (27%), leaving 73% without experimental validation.

The consequences are significant. First, simulation-only validation cannot capture real-world pneumatic brake delays, sensor noise, or thermal dynamics. Second, the absence of HIL/test bench validation reduces confidence in controller performance under extreme or emergency conditions. Third, commercial vehicle applications (with longer stopping distances and heavier loads) particularly require experimental validation.

Note: The 30.8% figure is based on the 39 representative studies; the trend is consistent across the full corpus.

4.8.4. Gap G6: Electrification-Specific Challenges

Severity: 7/10 and prevalence: 100% of studies involve electrified powertrains.

All 156 core papers address electric or hybrid vehicles, confirming that brake force distribution research is now fully embedded in the electrification context. However, several electrification-specific challenges remain unresolved despite the high prevalence. First, regenerative braking limits (battery state of charge, motor torque-speed characteristics, efficiency maps) are often simplified or ignored [9,14,34]. Second, combined regenerative-friction braking under emergency conditions remains challenging due to conflicting requirements (energy recovery vs. stability) [20,60,66]. Third, thermal coupling between electric motors, batteries, and brakes is rarely considered in a unified optimization framework [1,18,20,21].

The consequences are that current BFD controllers may overestimate energy recovery (ignoring battery/motor thermal limits), fail during regenerative-friction mode transitions, or compromise stability in favor of energy recuperation.

Note: 100% prevalence means every study in the corpus deals with electrified vehicles; this gap is defined by the unresolved challenges within this domain, not by the absence of coverage.

4.9. Research Gap Analysis Summary

The research gap analysis is summarized in Figure 12, which illustrates the six gaps (G1–G6) with severity scores (1–10) and prevalence percentages. The analysis confirms that Gap G2 (thermal-aware distribution) has the highest severity (10/10) and a prevalence of 97.4%, followed by Gap G1 (structural fragmentation) with severity 9/10 and a prevalence of 94.9%. These two gaps define the primary frontier for future research, motivating the hybrid MPC-PSO framework proposed in this work

5. Proposed Integrated Framework—The Test Rigor MPC-PSO System

The six research gaps identified in Section 4, particularly G2 (thermal-stability coupling) and G6 (electrification-specific challenges), motivate the design of a new hierarchical framework. This section proposes an MPC-PSO architecture with three control layers: PSO at 1–5 Hz for online weight adaptation, MPC at 20–50 Hz for constrained optimal control including thermal-state estimation, and an actuation layer at 100+ Hz.

5.1. Framework Overview and Design Philosophy

The proposed hierarchical MPC-PSO framework addresses the six research gaps (G1–G6) identified in Section 4 through a three-layer architecture that integrates adaptive parameter tuning (PSO), constrained optimal control (MPC), and physical validation on a dedicated test rig (test rigor).

The design philosophy rests on four principles. First, hierarchical decomposition separates slow adaptation (PSO, 1–5 Hz) from fast control (MPC, 20–50 Hz) to achieve real-time feasibility while maintaining adaptability [50,72]. Second, thermal-stability coupling explicitly incorporates brake thermal-state and friction-coefficient degradation into the MPC formulation, enabling real-time correction of the ideal distribution curve [1,21]. Third, a commercial vehicle focus addresses pneumatic actuator delays, extreme mass variation, and ECE-R13 compliance through model-based compensation and constraint formulation [22] by the application of cooperative braking through the magnetic brake and the effect of heat on it with the magnetic brake, the magnetic clutch, and the regenerative brake to measure the delay and achieve the best distribution between the front and rear axles. Fourth, physical validation is performed on a test rig that emulates regenerative braking, pneumatic actuators, and thermal loading under controlled laboratory conditions [14,63,84]. A conceptual illustration of the framework is provided in Figure 13.

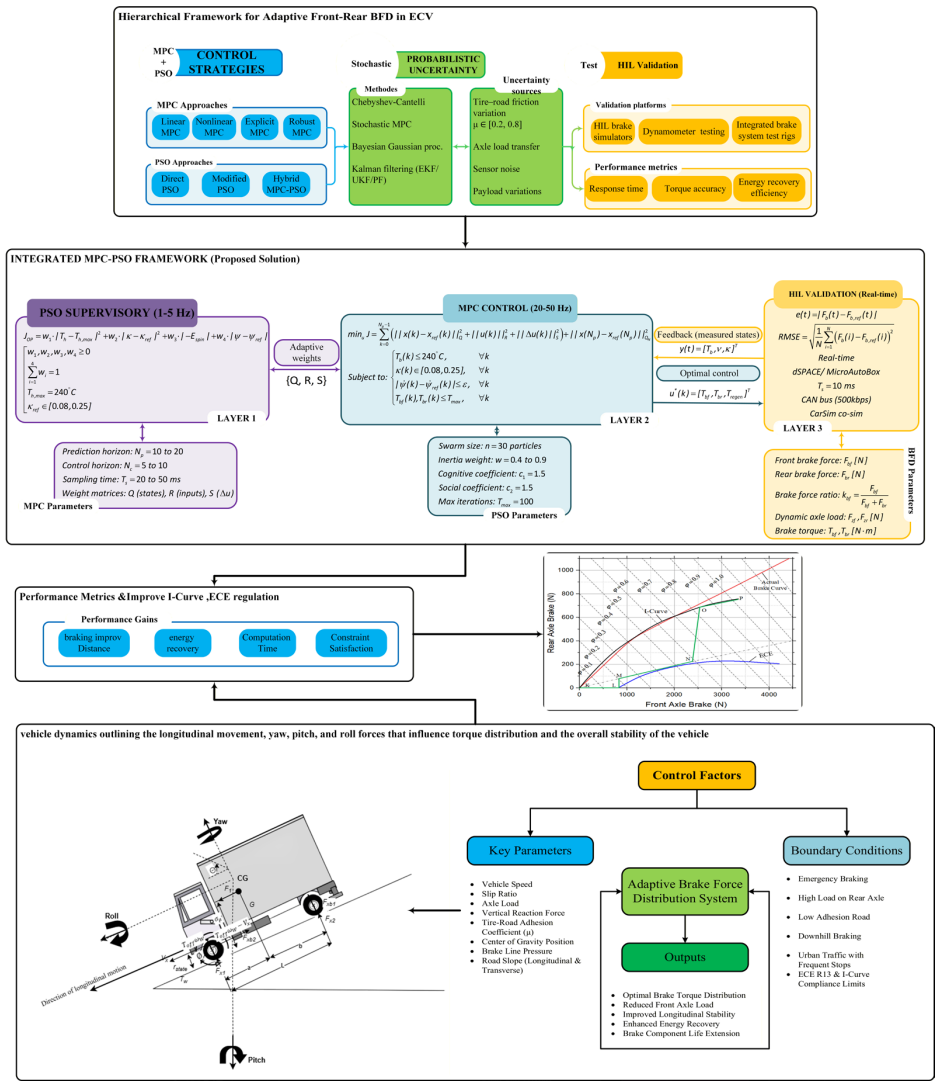


Figure 13. Hierarchical architecture of the proposed MPC PSO framework for adaptive front–rear brake force distribution.

5.2. Three-Layer Architecture

The proposed framework comprises three layers: Layer 1 (PSO-based adaptive parameter tuning, 1–5 Hz), Layer 2 (MPC-based constrained optimal control, 20–50 Hz), and Layer 3 (actuation and monitoring, 100+ Hz), as illustrated in Figure 13.

The three layers operate at different frequencies: Layer 1 (PSO, 1–5 Hz) optimizes MPC parameters; Layer 2 (MPC, 20–50 Hz) computes optimal brake forces subject to constraints; Layer 3 (actuation and HIL, >100 Hz) executes commands and monitors safety. The key mathematical formulations and the I-curve correction are indicated.

5.2.1. Layer 1: PSO-Based Adaptive (1–5 Hz)

The first layer employs particle swarm optimization (PSO) to adapt the MPC parameters in response to changing vehicle, thermal, and battery states. The inputs to this layer include the vehicle state (longitudinal velocity v, yaw rate r, sideslip angle β, axle loads F_{zf}, F_{zr}), the thermal state (front brake temperature T_f, rear brake temperature T_r, friction coefficients μ_f, μ_r), road conditions (slope θ, friction coefficient estimate μ_{road}), driver intent (brake pedal position δ_{brake}, deceleration request a_{req}), and battery state (state of charge (SOC), temperature T_{batt}, charge acceptance $P_{charge,max}$). The outputs are the MPC weighting matrices Q (state penalty) and R (control penalty), the constraint bounds $F_{bf,max}$, $F_{br,max}$, β_{max}, r_{max}, the prediction horizon N (10–50 steps), and the ideal curve correction factor of thermal correction factor $k_{thermal}$ (accounts for friction coefficient degradation).

The PSO solves the following multi-objective optimization problem:

$$\begin{aligned}
&\min J = \alpha \cdot E_{\text{regen}} + \beta \cdot t_{\text{stop}} + \gamma \cdot \beta_{\max} + \delta \cdot (T_f - T_{f,\text{target}})^2 + \varepsilon \cdot (T_r - T_{r,\text{target}})^2 \\
&\text{subject to :} \\
&1.\ \text{ECE-R13 distribution corridor compliance} \\
&2.\ \textit{Stability limits} : |\beta| \le \beta_{\max},\ |r| \le r_{\max} \\
&3.\ \textit{Thermal limits} :\ T_f \le T_{f,\max},\ T_r \le T_{r,\max} \\
&4.\ \textit{Regenerative torque limits} :\ T_{\text{regen}} \le T_{\text{motor,max}}(\omega, T_{\text{motor}}) \\
&5.\ \textit{Battery charge acceptance} :\ P_{\text{regen}} \le P_{\text{charge,max}}(T_{\text{batt}}, \text{SOC}) \\
&\text{where :} \\
&E_{\text{regen}} :\ \text{Regenerative energy recovered} \\
&t_{\text{stop}} :\ \text{Braking stopping time} \\
&\beta_{\max} : \text{Maximum sideslip angle} \\
&T_f, T_r :\ \text{Front and rear brake temperatures} \\
&T_{f,\text{target}}, T_{r,\text{target}} :\ \text{Target brake temperatures} \\
&T_{\text{regen}} :\ \text{Regenerative braking torque} \\
&P_{\text{regen}} : \text{Regenerative braking power} \\
&\alpha, \beta, \gamma, \delta, \varepsilon : \text{Weighting coefficients} n
\end{aligned} \tag{11}$$

The PSO algorithm maintains a swarm of 20–50 particles, each representing a candidate set of MPC parameters (Q, R, N, $k_{thermal}$). The swarm is initialized with parameters from a pre-trained lookup table based on vehicle speed, load, and thermal state. The PSO algorithm iterates for 10–20 iterations (0.2–1.0 s at 1–5 Hz update rate), converging to a locally optimal parameter set that is passed to Layer 2 [29,32,82,83].

5.2.2. Layer 2: MPC-Based Constrained Optimal Control (20–50 Hz)

The second layer receives the vehicle state (longitudinal vehicle state: $v, r, \beta,\ F_{zf}, F_{zr}$), the thermal state (brake temperatures T_f, T_r, μ_f, μ_r), the PSO-tuned parameters (Q, R, N, $k_{thermal}$), and the driver deceleration request a_{req}. It computes the front and rear brake force commands (F_{bf}, F_{br}) and the regenerative braking torque command (T_{regen}) by solving a constrained finite-horizon optimal control problem.

The MPC optimization is subject to the following constraints:

$$\min \sum_{i=0}^{N-1} \left[(v_{k+i\,|\,k} - v_{\text{ref}})^2 \cdot q_v + r_{k+i|k}^2 \cdot q_r + \beta_{k+i|k}^2 \cdot q_\beta + F_{bf,k+i|k}^2 \cdot r_{bf} + F_{br,k+i|k}^2 \cdot r_{br} \right] \quad (12)$$

The MPC optimization is solved using sequential quadratic programming (SQP) or interior-point methods, with a prediction horizon of N = 10–50 steps (0.2–1.0 s at 20–50 Hz sampling). The thermal correction factor $k_{thermal}$ adjusts the ideal curve constraint based on real-time friction coefficient estimates, enabling dynamic redistribution to compensate for brake fade [20,21,80,81].

5.2.3. Layer 3: Actuation and Monitoring (100+ Hz)

The lowest layer executes the brake force commands at a high update rate (>100 Hz) and monitors system health. It receives the front and rear brake force commands F_{bf}, F_{br} and the regenerative torque command T_{regen} from Layer 2, and produces the pneumatic brake pressures P_f, P_r, the motor torque command T_{motor}, as well as fault-detection flags for actuator saturation, sensor faults, and thermal runaway. The actuation and monitoring functions comprise five tasks. Actuator control uses a proportional-integral (PI) controller with feedforward compensation for the inherent delay (≈80–120 ms). Regenerative braking control implements motor torque limiting with current and thermal protection. Sensor fusion applies a Kalman filter to estimate the vehicle state (velocity, yaw rate, sideslip angle) from wheel speed sensors, an IMU, and GPS. Fault detection relies on model-based residual generation to identify actuator faults, sensor abnormalities, and thermal overload. Finally, safety interlocks provide emergency stopping, actuator saturation detection, and enforcement of thermal limits. These high-rate functions ensure that the optimized brake forces are realized safely and reliably on the physical test rig.

As a systematic review, this paper does not present new experimental data. Its achieved outcomes are the identification, quantification, and theoretical synthesis of research gaps, together with the proposal of a validated framework architecture that directly addresses those gaps. Specifically, the review delivers: (i) a PRISMA-compliant quantification of tripartite fragmentation across 156 core studies; (ii) a five-group taxonomic classification; (iii) six explicit research gaps (G1–G6) with severity and prevalence scores; (iv) a three-layer hierarchical control architecture (PSO: 1–5 Hz, MPC: 20–50 Hz, actuation: 100+ Hz); and (v) a detailed test rig specification for physical validation.

The proposed framework offers clear comparative advantages over existing methods, whereas MPC-only studies add online PSO weight adaptation (real-time tuning), PSO-only studies add real-time MPC constraint handling (safety guarantees), previous integrated frameworks uniquely couple thermal-state estimation with real-time control (absent in all 156 core studies), and all existing studies provide a test rig specification (thermal sensing, eddy current retarders and magnetic brakes, ECE-R13 compliance), enabling future experimental validation. Thus, the proposed framework advances the state of the art by synthesizing fragmented knowledge, filling six explicit research gaps.

5.3. Test Rigor Test Rig Architecture

The proposed framework will be validated on a physical test rig that emulates the dynamics of a 5-ton electric commercial vehicle with front axle regenerative braking, eddy current retarder with rear axle, and magnetic brakes on both axles. The test rig comprises several subsystems, as shown in Figure 14:

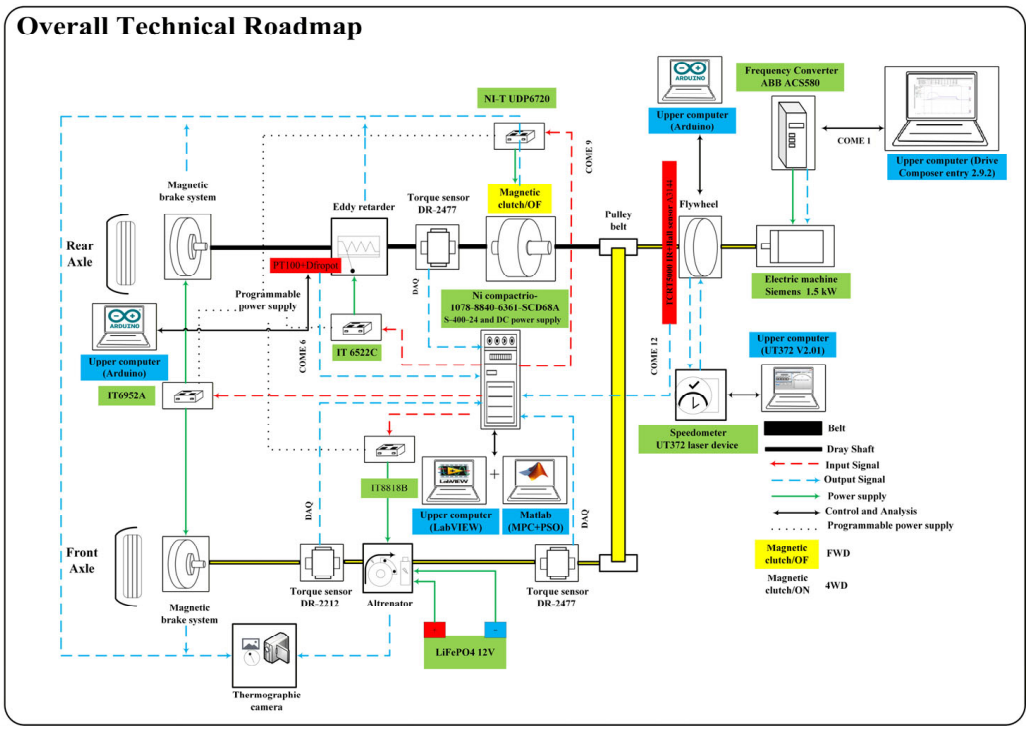


Figure 14. Experimental test rig architecture for validation of the hierarchical MPC-PSO framework.

The proposed framework will be validated on a dedicated test rig (test rigor) that emulates the longitudinal dynamics of an electric commercial vehicle. The rig integrates front axle regenerative braking with a magnetic brake system that emulates pneumatic friction brakes on both axles. It comprises subsystems: regenerative braking emulation (IT6952A), torque sensing (DR-2212/DR-2477), thermal sensing (PT100 + DFRobot), real-time control (NI CompactRIO), electric motor emulation (Siemens PMSM + ABB ACS580), energy storage ($LiFePO_4$), speed sensing (UT372 + TCRT5000), co-simulation (LabVIEW 2023 + MATLAB R2023b), and safety systems.

5.3.1. Regenerative Braking Emulation

Regenerative braking is implemented on a physical test rig consisting of a belt-driven alternator connected to the shaft. The alternator output is rectified and fed to a 12 V $LiFePO_4$ battery in parallel with an IT8818B regenerative DC electronic load (ITECH). The load can continuously sink 1.5 kW (1.8 kW peak for 30 s) and is programmable in voltage and current via Modbus RTU or analog 0–10 V. Recovered energy is primarily stored in the battery, while the IT8818B optionally dissipates or returns excess energy to the grid. Alternator speed is derived from the measured rear shaft speed (Hall sensor/tachometer) and the pulley diameter ratio. Instantaneous charging current and voltage are measured by a Hall effect sensor and a voltage divider, respectively, and logged synchronously with torque sensors, PT100 (ECR temperature), TCR5000 signals, and clutch status (ON/OFF via ABB ACS580 at 5–30 Hz) into LabVIEW through an Arduino interface. This setup enables quantification of instantaneous regenerative power $P_{regen}(t) = V(t) \cdot I(t)$, recovered energy $E_{regen} = \int Pregen.dt$, and the contribution of regenerative braking to overall brake force distribution under different operating modes (MB-only, ECR-only, MB + ECR, MB + Regen, and MB + ECR + Regen).

5.3.2. Magnetic Brake Actuation and Eddy Current Retarder

Instead of pneumatic brakes, the test rig employs a magnetic brake system that combines a magnetic clutch (engagement/disengagement) and a magnetic retarder (eddy

current brake). This configuration allows continuous modulation of the braking torque under closed-loop control. The magnetic brake force is regulated based on the driver's deceleration request and the real-time thermal state of the clutch, measured by PT100 sensors. A feedforward-plus-PI controller compensates for the thermal-dependent friction behavior, ensuring that the front–rear brake force distribution follows the desired (thermal-corrected) I-curve. The magnetic brake system thereby emulates the key characteristics of commercial vehicle pneumatic brakes, namely time delay, the nonlinear force–pressure relationship, and thermal sensitivity without requiring compressed air.

5.3.3. Thermal Sensing and Emulation

Brake temperatures are measured by PT100 resistance thermometers (Class A, ±0.15 °C at 0 °C) placed on the rear brake disks of the eddy current retarder (ECR). The PT100 signals are conditioned via a voltage divider (DFRobot) and acquired through an Arduino UNO3 interface into LabVIEW. Additionally, a thermographic camera (0–1000 °C, ±1%) monitors surface temperature distribution on the ECR, magnetic powder brakes, and bearings. The measured temperatures are used to validate thermal constraints in the brake force distribution model and to prevent overheating during prolonged braking tests.

The ECR is controlled by an IT6522C power supply (60 V DC, 0.2–4 A or 0.5–4 A adjustable), based on torque sensor readings, temperature feedback (PT100), and other synchronized signals (TCR5000, Hall sensor, speed). The rear shaft speed is regulated by an ABB ACS580 frequency converter (5, 10, 15, 20, 25, 30 Hz) via a magnetic clutch (ON/OFF). This setup enables the evaluation of regenerative braking efficiency and optimal brake torque distribution between front and rear axles using integrated MPC-PSO control.

5.3.4. Real-Time Control and Data Acquisition

Real-time control is executed on an NI CompactRIO-9030 controller, powered by a 24 V DC supply (S-400-24). The I/O complement includes analog inputs (NI-9205), analog outputs (NI-9263), digital I/O (NI-9401), and serial communication (NI-9870). The controller operates the MPC at 50 Hz, the actuation loop at 100 Hz, and data acquisition at 1 kHz, satisfying the hierarchical timing requirements of the framework, which satisfies the real-time requirements for slip calculation, torque–current characterization, and brake force distribution optimization.

5.3.5. Electric Motor and Drivetrain Emulation

A Siemens three-phase induction motor (1.5 kW rated power, 3000 rpm rated speed) is used to emulate the axle electric drive. The motor is controlled by an ABB ACS580 variable frequency drive (2.2 kW), which operates in speed control mode (V/f). The drive is programmed via Drive Composer 2.9.2 software running on an upper computer, allowing the user to set discrete frequency steps (1–30 Hz). From the drive, the following quantities are logged: motor frequency command, actual speed (rpm), phase current, input voltage, input power, power factor ($cos\varphi$), estimated efficiency, and motor temperature. This setup enables: (i) comparative analysis of braking strategies (magnetic brake, magnetic clutch, ECR, regenerative braking) with MPC-PSO; (ii) conversion of mechanical shaft speed to equivalent vehicle speed coupled with a half-car model; (iii) calculation of input vs. recovered/lost power; (iv) analysis of drivetrain stability during braking (torque ripple, saturation, mechanical imbalance); and (v) integration with the physical rig where the motor acts as the propulsion unit, the flywheel represents vehicle inertia, and the shafts, magnetic brakes, eddy current retarder, regenerative alternator, and magnetic clutch represent the full braking system.

5.3.6. Energy Storage Emulation

A 12 V $LiFePO_4$ battery (actual capacity, e.g., 50 Ah) stores energy recovered during regenerative braking. The alternator output, rectified to ≈13 V, charges the battery via a parallel connection with an IT8818B regenerative DC electronic load (1.5 kW continuous). Charging voltage and current are measured using a Hall sensor and voltage divider, logged via LabVIEW. Regenerative power and energy are computed online, enabling efficiency analysis against mechanical braking torque (MB/ECR). No external BMS is used; current is limited by the IT8818B to safe values.

5.3.7. Speed and Position Sensing

The rotational speed of the flywheel, which represents the equivalent vehicle inertia, is measured using a UT372 non-contact laser tachometer (±0.05%). The tachometer is positioned at a fixed distance of 0.5 m from the flywheel surface and provides speed readings every 0.5 s, transmitted to an upper computer via the UT372 V2.01 software. The measured speed (rpm) is converted to angular velocity ω (rad/s). From the time history $\omega(t)$ during acceleration and braking (using MB, ECR, or regenerative braking), the angular acceleration $\alpha = d\omega/dt$ is derived, which gives the deceleration rate (jerk) and enables calculation of the actual braking torque applied by each brake type:

$$T_{brake} = I_{flywheel} \cdot \alpha \tag{13}$$

where $I_{flywheel} \approx 0.96$ kg·m^2 (calculated from the measured geometry and mass of the flywheel). The stopping time and the dissipated/recovered energy are also obtained from $\omega(t)$.

Road condition detection is performed using two TCRT5000 reflective optical sensors. One sensor distinguishes between two colors representing straight/flat road (e.g., white/black pattern), and the other sensor distinguishes between slippery (ice) and asphalt surfaces via a colored track. The binary outputs of these sensors are acquired by an Arduino UNO3 and sent to LabVIEW through an NI cRIO-9030 (with the identifier 1078-8840-6361-SCD68A). The road-type parameter is fed into the MPC + PSO controller to adapt the brake force distribution.

Wheel speeds (for slip ratio calculation) are obtained from A3144 Hall effect sensors mounted near the front and rear wheels. Alternatively, the TCRT5000 sensors can be configured as incremental encoders (60 pulses per revolution, 5 µs response time) to provide wheel speed information. The Hall sensors also provide a pulse output proportional to rotational speed, acquired via the Arduino and cRIO.

Additionally, a magnetic clutch (controlled by a LabVIEW-driven NI-T UDP6720 device) is placed at the beginning of the rear shaft. The clutch allows switching between front-wheel drive (FWD) and all-wheel drive modes. Its torque–current characteristic is mapped at various speeds, and its engagement/disengagement time is measured for emergency braking scenarios (ABS/ESC compatibility). The clutch status (ON/OFF) is used as a parameter in the brake force distribution logic, based on speed, torque sensor readings (DR-2477), TCRT5000 road condition, and PT100 temperature feedback.

All sensor signals (UT372, TCRT5000, Hall, torque sensors, PT100, clutch status) are synchronously acquired via Arduino, LabVIEW, and NI cRIO at a sampling rate of 1 kHz, enabling real-time state estimation, slip ratio computation, and closed-loop control.

5.3.8. Software and Co-Simulation

The real-time control (MPC, actuation, monitoring) is implemented in LabVIEW 2023 Real-Time and deployed on the Compact RIO, running the MPC at 50 Hz and actuation at 100 Hz. Offline PSO and vehicle dynamics simulation are performed in MATLAB/Simulink

R2023b. Parameter updates (1 Hz) from the PSO to the MPC are exchanged via TCP/IP socket communication between LabVIEW and MATLAB.

5.3.9. Safety and Fault Detection

Safety and fault detection are enforced at three levels. Hardware interlocks include an emergency stop (hardwired to the magnetic brake power supply and motor drive), thermal runaway detection (emergency stop if brake temperature exceeds 240 °C), and actuator saturation detection. Algorithmic detection uses model-based residual generation for actuator faults, Kalman filter innovation for sensor faults, and a thermal model to detect brake fade (comparison of estimated friction coefficient with measured deceleration).

5.4. Merits and Limitations of the Proposed Framework

The proposed hierarchical MPC-PSO framework exhibits five principal merits. First, it directly addresses all six research gaps (G1–G6) identified in Section 4: integration of control and optimization paradigms (G1, G4), real-time thermal-aware distribution (G2), focus on commercial vehicles with actuators (G3), physical test-rig validation (G5), and electrification-specific challenges through battery–thermal–electrical coupling (G6). Second, real-time feasibility is achieved by decoupling slow adaptation (PSO, 1–5 Hz) from fast control (MPC, 20–50 Hz), enabling implementation on embedded hardware (NI CompactRIO) while maintaining adaptability [50,72]. Third, formal constraint satisfaction, including stability limits, actuator saturation, and ECE-R13 ideal curve compliance, is guaranteed by the MPC formulation, addressing the safety-critical nature of brake force distribution [80,81]. Fourth, thermal-stability coupling via the correction factor $k_{thermal}$ dynamically adjusts the ideal distribution curve based on real-time friction coefficient estimates, compensating for brake fade during sustained braking [1,21]. Fifth, the framework explicitly accounts for actuator delays, extreme mass variation, and ECE-R13 compliance, filling a critical gap in the commercial vehicle literature [22].

5.5. Limitations

Despite these merits, five limitations are acknowledged. First, the test rig emulates a 5-ton commercial vehicle at reduced scale (1.5 kW front axle drive motor vs. 150 kW full-scale motor), limiting the fidelity of thermal loading and regenerative braking dynamics, particularly for the belt-driven alternator on the rear axle (1.5 kW continuous); full-scale validation on a commercial vehicle test track is required for industrial deployment. Second, the MPC formulation employs a simplified linear tire model with a constant friction coefficient, neglecting temperature, wear, and pressure variations; more accurate nonlinear tire models would improve fidelity but increase computational cost. Third, regenerative braking is implemented only on the front axle via the alternator (12 V $LiFePO_4$ battery and IT8818B load), which matches the physical test rig, whereas dual axle regeneration (front + rear) would require an additional motor/generator on the front axle and a more complex control allocation. Fourth, the PSO algorithm is initialized with parameters from a pre-trained lookup table, requiring offline training on representative driving cycles; online learning or adaptive initialization would improve robustness under novel conditions but increase real-time computational load. Fifth, the MPC formulation assumes deterministic vehicle dynamics and road conditions, neglecting stochastic disturbances such as road roughness, wind gusts, and sensor noise; stochastic MPC or robust MPC formulations would enhance robustness at the expense of higher computational cost.

6. Conclusions

This PRISMA-2020-compliant systematic review of 156 core papers (2016–2026) reveals a structural tripartite fragmentation: thermal management, real-time brake force redistri-

bution, and stability-constrained optimal control are treated separately. Only four studies explicitly integrate MPC and PSO, and only four studies incorporate thermal constraints; no study addresses ECE-R13 compliance or laden/unladen load adaptation. Six research gaps (G1–G6) have been quantified (severity 8–10/10, prevalence 61–100%). To address these gaps, a hierarchical MPC-PSO framework is proposed (Layer 1: PSO, 1–5 Hz; Layer 2: MPC, 20–50 Hz; Layer 3: actuation/monitoring, >100 Hz). The framework corrects the ideal distribution curve in real time using a thermal factor $k_{thermal}$ and explicitly accounts for braking delays and load variation.

The main theoretical contributions are: (i) the first PRISMA-compliant review focused on adaptive BFD with thermal constraints for commercial vehicles; (ii) a taxonomy of five thematic groups (A–E) and six quantified research gaps; (iii) the demonstration that a hierarchical MPC-PSO architecture is the most promising unified solution; and (iv) the introduction of a thermal correction factor for real-time I-curve adjustment. The practical contributions include: (i) a detailed test rigor test rig architecture; (ii) a three-phase validation protocol; (iii) five merits and five limitations of the proposed framework; and (iv) a roadmap for industrial deployment.

Policy implications. Three policy recommendations emerge. First, ECE-R13 Annex 10 should be revised to require that brake force distribution remain within the permissible corridor under sustained braking (e.g., 6% grade, 10 km, at gross vehicle weight). Thermal monitoring and brake-fade warning systems should be mandatory for vehicles > 12 t. Second, minimum performance requirements for regenerative braking should be established to ensure that thermal limits are not exceeded during sustained braking. Third, public–private research partnerships should prioritize validation of hierarchical MPC-PSO frameworks on physical test rigs and the development of industry-standard test protocols. These measures will accelerate the safe electrification of commercial vehicle fleets.

Supplementary Materials: The following supporting information can be downloaded at: https://www.mdpi.com/article/10.3390/app16125786/s1, Table S1: PRISMA 2020 Checklist; Table S2: PRISMA 2020 for Abstract Checklist.

Author Contributions: Conceptualization, A.Y.A. and G.T.; methodology, A.Y.A.; formal analysis, A.Y.A.; investigation, A.Y.A.; visualization, A.Y.A. and E.K.M.M.; writing—original draft preparation, A.Y.A.; writing—review and editing, A.Y.A., A.J.F., E.K.M.M., J.V.F. and H.W.; supervision, G.T. All authors have read and agreed to the published version of the manuscript.

Funding: This research was funded by the special funds of the Department of Emergency Management of Hubei Province, China, and the hazardous chemicals liquid transportation rescue vehicle (2021YJT014). The systematic literature review was conducted as part of doctoral research at [Suizhou-WUT Industry Research Institute/Wuhan University of Technology].

Institutional Review Board Statement: Not applicable.

Informed Consent Statement: Not applicable.

Data Availability Statement: No new data were created or analyzed in this study.

Acknowledgments: The authors acknowledge the use of the IEEE Xplore Digital Library and Web of Science Core Collection for systematic literature search and wish to acknowledge the Suizhou-WUT Industry Research Institute, Hubei Key Laboratory of Advanced Technology for Automotive Components, Hubei Collaborative Innovation Centre for Automotive Components Technology, Wuhan University of Technology, Wuhan 430070, China, and Suizhou-WUT Industry Research Institute, Suizhou 441300, China.

Conflicts of Interest: The authors declare no conflicts of interest.

Nomenclature

$V_{k+i\|k}$	Predicted longitudinal velocity at horizon i (m/s)
V_{ref}	Reference (desired) velocity (m/s)
$r_{k+i\|k}$	Predicted yaw rate at horizon i (rad/s)
$\beta_{k+i\|k}$	Predicted sideslip angle at horizon i (rad)
$F_{b,f,k+i\|k}$	Predicted front brake force at horizon i (N)
$F_{b,r,k+i\|k}$	Predicted rear brake force at horizon i (N)
q_v	Velocity error weighting coefficient (-)
q_r	Yaw rate weighting coefficient (-)
q_β	Sideslip angle weighting coefficient (-)
$r_{b,f}$	Front brake force weighting coefficient (-)
$r_{b,r}$	Rear brake force weighting coefficient (-)
N	Prediction horizon (-)
$v(k)$	Longitudinal velocity at time step k (m/s)
$F_{bf}(k)$	Front brake force at time step k (N)
$F_{br}(k)$	Rear brake force at time step k (N)
$F_{drag}(k)$	Aerodynamic drag force (N)
$F_{grade}(k)$	Grade resistance force (N)
m	Vehicle mass (kg)
Δt	Sampling time (control step) (s)
r(k)	Yaw rate at time step k (rad/s)
I_z	Yaw moment of inertia (kg·m)
$F_{yf}(k)$	Front tire lateral force at time step k (N)
$F_{yr}(k)$	Rear tire lateral force at time step k (N)
I_f	Distance from CG to front axle (m)
I_r	Distance from CG to rear axle (m)
β_k	Sideslip angle at time step k (rad)
$k_{thermal}(k)$	Thermal correction factor $(0 \leq k_{thermal} \leq 1)$ (-)
$F_{ideal}(\cdot)$	Ideal ECE-R13 brake force distribution function (N)
$F_{zf}(k)$	Front axle vertical load (N)
$F_{zr}(k)$	Rear axle vertical load (N)
$F_{bf,max}(k)$	Maximum allowable front brake force (N)
$\beta_{max}(k)$	Maximum allowable sideslip angle (rad)
$r_{max}(k)$	Maximum allowable yaw rate (rad/s)
$F_{br,\,actual}(t)$	Actual rear brake force at time t (N)
$F_{br,\,cmd}(t)$	Commanded rear brake force at time t (N)
T_{delay}	Actuator delay (s)
$F_{br,max}$	Maximum rear brake force (N)
λ_f,λ_r	Longitudinal slip (front/rear) (-)
λ_{min},λ_{max}	Slip limits (-)
ΔF_{max}	Maximum brake force rate (N/s)
T_{regen}	Regenerative braking torque (EV) (Nm)
$T_{motor,max}$	Maximum motor torque (EV) (Nm)
ω	Motor angular speed (EV) (rad/s)
$X_{k+i\|k} \in R^n$	State vector at step $k+i$ (Slip, velocity, torque, etc.)
$U_{k+i\|k} \in R^m$	Control vector (front/rear brake force) (N)
$d_{k+i\|k} \in R^p$	Disturbance vector (road slope, friction) (-)
$Q \in R^{n\times n}$	State weighting matrix $(Q \geq 0)$
$R \in R^{m\times m}$	Control weighting matrix $(R > 0)$
$P \in R^{n\times n}$	Terminal cost matrix $(Riccati\ equation\ solution)$
F_{total}	Ideal brake force distribution curve (ECE-R13) (N)

References

1. Xin, T.; Xu, J. A Data- and Model-Integrated Driven Method for Recommending the Maximum Safe Braking Deceleration Rates for Trucks on Horizontal Curves. *Appl. Sci.* **2024**, *14*, 9357. [CrossRef]
2. Zheng, W.; Chen, J.; Wang, S. Research on an Energy Recovery Strategy for Fuel Cell Commercial Vehicles Based on Slope Estimation. *Appl. Sci.* **2024**, *14*, 748. [CrossRef]
3. Caponio, C.; Tavolo, G.; Tavernini, D.; Karci, A.E.H.; Ahmadi, J.; Lenzo, B.; Reina, G.; Mantriota, G.; Perlo, P.; Sorniotti, A. Nonlinear Model Predictive Yaw Moment Control Through Electric Axle and Friction Brake Torque Distribution. *IEEE Access* **2025**, *13*, 106540–106560. [CrossRef]
4. Economic Commission for Europe of the United Nations (UNECE). Regulation No 13 of the Economic Commission for Europe of the United Nations (UN/ECE)—Uniform Provisions Concerning the Approval of Vehicles of Categories M, N and O with Regard to Braking. 2016. Available online: https://eur-lex.europa.eu/eli/reg/2016/194/oj (accessed on 10 May 2026).
5. Zhang, L.; Yu, L.; Wang, Z.; Zuo, L.; Song, J. All-Wheel Braking Force Allocation During a Braking-in-Turn Maneuver for Vehicles with the Brake-by-Wire System Considering Braking Efficiency and Stability. *IEEE Trans. Veh. Technol.* **2016**, *65*, 4752–4767. [CrossRef]
6. Limpert, R. *Brake Design and Safety*, 3rd ed.; SAE International: Warrendale, PA, USA, 2011; ISBN 978-0-7680-5789-8.
7. Ruan, J.; Walker, P.D.; Watterson, P.A.; Zhang, N. The Dynamic Performance and Economic Benefit of a Blended Braking System in a Multi-Speed Battery Electric Vehicle. *Appl. Energy* **2016**, *183*, 1240–1258. [CrossRef]
8. Subramaniyam, K.V.; Subramanian, S.C. Analysis of Cornering Response and Stability of Electrified Heavy Commercial Road Vehicles with Regenerative Braking. *Proc. Inst. Mech. Eng. Part D J. Automob. Eng.* **2020**, *234*, 1672–1689. [CrossRef]
9. Li, W.; Du, H.; Li, W. Four-Wheel Electric Braking System Configuration with New Braking Torque Distribution Strategy for Improving Energy Recovery Efficiency. *IEEE Trans. Intell. Transp. Syst.* **2020**, *21*, 87–103. [CrossRef]
10. Sun, C.; Chu, L.; Guo, J.; Shi, D.; Li, T.; Jiang, Y. Research on Adaptive Cruise Control Strategy of Pure Electric Vehicle with Braking Energy Recovery. *Adv. Mech. Eng.* **2017**, *9*, 168781401773499. [CrossRef]
11. Chu, L.; Li, J.; Liu, M.; Wang, Y.; Jiang, Z.; Guo, C. A Nonlinear Explicit Model Predictive Controller for an Electro-Hydraulic Braking System of an Electric Vehicle Driven by a Four-Wheel Hub. In *Proceedings of the 2023 7th CAA International Conference on Vehicular Control and Intelligence (CVCI)*; IEEE: Changsha, China, 2023; pp. 1–8.
12. Techalimsakul, P.; Keyoonwong, W. Integrated Vehicle-Following Control for Four-Wheel Independent Drive Based on Regenerative Braking System Control Mechanism for Battery Electric Vehicle Conversion Driven by PMSM 30 kW. *Energies* **2024**, *17*, 2576. [CrossRef]
13. He, C.; Wang, G.; Gong, Z.; Xing, Z.; Xu, D. A Control Algorithm for the Novel Regenerative–Mechanical Coupled Brake System with by-Wire Based on Multidisciplinary Design Optimization for an Electric Vehicle. *Energies* **2018**, *11*, 2322. [CrossRef]
14. Fajri, P.; Lee, S.; Prabhala, V.A.K.; Ferdowsi, M. Modeling and Integration of Electric Vehicle Regenerative and Friction Braking for Motor/Dynamometer Test Bench Emulation. *IEEE Trans. Veh. Technol.* **2016**, *65*, 4264–4273. [CrossRef]
15. Nanda Kumar, C.; Subramanian, S.C. Brake Force Sharing to Improve Lateral Stability While Regenerative Braking in a Turn. *Proc. Inst. Mech. Eng. Part D J. Automob. Eng.* **2019**, *233*, 531–547. [CrossRef]
16. Li, X.; Ma, J.; Zhao, X.; Wang, L. Study on Braking Energy Recovery Control Strategy for Four-Axle Battery Electric Heavy-Duty Trucks. *Int. J. Energy Res.* **2023**, *2023*, 1868528. [CrossRef]
17. Liu, W.; He, H.; Sun, F.; Lv, J. Integrated Chassis Control for a Three-Axle Electric Bus with Distributed Driving Motors and Active Rear Steering System. *Veh. Syst. Dyn.* **2017**, *55*, 601–625. [CrossRef]
18. Li, W.; Song, Z.; Ding, H.; Xu, N. Energy-Efficient Predictive and Reactive Control of Connected Electric Vehicles Platoon with String Stability Based on Variable Time Headway. *IEEE Trans. Transp. Electrif.* **2025**, *11*, 1970–1983. [CrossRef]
19. Wang, Y.; Zhou, L.; Chu, L.; Zhao, D.; Guo, Z.; Jiang, Z. A Multi-Source Braking Force Control Method for Electric Vehicles Considering Energy Economy. *Energies* **2024**, *17*, 2032. [CrossRef]
20. Belloni, M.; Bracaccia, L.; Vignati, M.; Tarsitano, D. Thermomechanical Model Predictive Cascade Control for Blended Braking of an IWM Vehicle. In *Proceedings of the 2023 IEEE Vehicle Power and Propulsion Conference (VPPC)*; IEEE: Milan, Italy, 2023; pp. 1–6.
21. Sun, T.; Yang, C.; Zhang, M.; Wang, W. An Efficient Braking Energy Recovery Strategy Based on Differential Game for Hybrid Electric Truck Considering Electromechanical Thermal Dynamic. In *Proceedings of the 2023 7th CAA International Conference on Vehicular Control and Intelligence (CVCI)*; IEEE: Changsha, China, 2023; pp. 1–6.
22. Gautam, V.; Rajaram, V.; Subramanian, S.C. Model-Based Braking Control of a Heavy Commercial Road Vehicle Equipped with an Electropneumatic Brake System. *Proc. Inst. Mech. Eng. Part D J. Automob. Eng.* **2017**, *231*, 1693–1708. [CrossRef]
23. Alizadehghobadi, S.; Ehsani, R. Robust Invariant Set Design for Reliable Stopping in Adaptive Cruise Control via Model Predictive Control. *IEEE Access* **2025**, *13*, 81096–81104. [CrossRef]
24. Zhao, Y.; Yang, Y. Pressure Control for Pneumatic Electric Braking System of Commercial Vehicle Based on Model Predictive Control. *IET Intell. Transp. Syst.* **2021**, *15*, 1522–1532. [CrossRef]

25. Xing, C.; Zhu, Y.; Wang, J.; Lin, Y. Braking Torque Distribution Reconfiguration Strategy of Vehicle with Faults of In-Wheel Motor Drive System. *IEEE Trans. Intell. Transp. Syst.* **2024**, *25*, 14476–14485. [CrossRef]
26. Xu, Q.; Wu, S. Design of Regenerative Braking Strategy for Hybrid Electric Vehicle Based on Sensitivity Ratio. In *Proceedings of the 2023 35th Chinese Control and Decision Conference (CCDC)*; IEEE: Yichang, China, 2023; pp. 1209–1214.
27. Liu, H.; Lei, Y.; Fu, Y.; Li, X. Multi-Objective Optimization Study of Regenerative Braking Control Strategy for Range-Extended Electric Vehicle. *Appl. Sci.* **2020**, *10*, 1789. [CrossRef]
28. Wu, J.; Liu, H.; Ren, X.; Nie, S.; Qin, Y.; Han, L. A Multi-Objective Optimization Approach for Regenerative Braking Control in Electric Vehicles Using MPE-SAC Algorithm. *Energy* **2025**, *318*, 134586. [CrossRef]
29. Zhu, Y.; Wu, H.; Zhen, C. Regenerative Braking Control under Sliding Braking Condition of Electric Vehicles with Switched Reluctance Motor Drive System. *Energy* **2021**, *230*, 120901. [CrossRef]
30. Zheng, Z.; Liang, C. Research on Particle Swarm Optimization Algorithm of Electromechanical Hybrid Braking Control Strategy Based on Road Surface Recognition. *Energy Sources Part A Recovery Util. Environ. Eff.* **2025**, *47*, 2027580. [CrossRef]
31. Zhu, Y.; Wu, H.; Zhang, J. Regenerative Braking Control Strategy for Electric Vehicles Based on Optimization of Switched Reluctance Generator Drive System. *IEEE Access* **2020**, *8*, 76671–76682. [CrossRef]
32. Anselma, P.G.; Belingardi, G. Multi-Objective Optimal Computer-Aided Engineering of Hydraulic Brake Systems for Electrified Road Vehicles. *Veh. Syst. Dyn.* **2022**, *60*, 391–412. [CrossRef]
33. Kopczyński, A. Active Torque Distribution Strategy for Electric Vehicle Independent Axle Drive. *E3S Web Conf.* **2019**, *100*, 00037. [CrossRef]
34. Zhi, J.; Wang, X.; Shi, Q.; Yao, Z.; Qi, Y. Torque Allocation Strategy Based on Economy and Stability for Electric Vehicle Considering Controllability after Motors Failure. *Proc. Inst. Mech. Eng. Part D J. Automob. Eng.* **2023**, *237*, 2759–2779. [CrossRef]
35. Luo, C.; Yang, Y.; Zhong, Z. Optimal Braking Torque Distribution of Dual-Motor Front-Rear Individually Driven Electric-Hydraulic Hybrid Powertrain Based on Minimal Energy Loss. *IEEE Access* **2022**, *10*, 134404–134416. [CrossRef]
36. Xu, Y.; Jiang, L.; Wei, B.; Qiu, L. An Optimal Torque Distribution Strategy for Four-Motorized-Wheel Electric Vehicle Considering Energy Conversation. *IEEE Access* **2020**, *8*, 135975–135988. [CrossRef]
37. Zhao, X.; Guo, G. Braking Torque Distribution for Hybrid Electric Vehicles Based on Nonlinear Disturbance Observer. *Proc. Inst. Mech. Eng. Part D J. Automob. Eng.* **2019**, *233*, 3327–3341. [CrossRef]
38. Tan, Z.; Wang, H.; Cheng, W.; Peng, X.; Yi, C.; Deng, L.; Wang, X. Power Optimization Control Strategy for Dual Motor Multi-Axis Drive Autonomous Vehicles. *Sci. Tech. Energy Transit.* **2025**, *80*, 51. [CrossRef]
39. Huang, B.; Wei, J.; Ma, M.; Yang, X. Research on Energy-Saving Optimization Control Strategy for Distributed Hub Motor-Driven Vehicles. *Energies* **2025**, *18*, 3025. [CrossRef]
40. Lv, C.; Zhang, J.; Li, Y.; Yuan, Y. Mechanism Analysis and Evaluation Methodology of Regenerative Braking Contribution to Energy Efficiency Improvement of Electrified Vehicles. *Energy Convers. Manag.* **2015**, *92*, 469–482. [CrossRef]
41. Zhang, X.; Göhlich, D. Integrated Traction Control Strategy for Distributed Drive Electric Vehicles with Improvement of Economy and Longitudinal Driving Stability. *Energies* **2017**, *10*, 126. [CrossRef]
42. Kumar, D.P.; Gupta, S.; Suriyamoorthy, S.; Subramanian, S.C. Design of a Dynamic Brake Force Regulation Strategy for Heavy Commercial Road Vehicles. In *Proceedings of the TENCON 2019—2019 IEEE Region 10 Conference (TENCON)*; IEEE: Kochi, India, 2019; pp. 643–648.
43. Dong, H.; Zhuang, W.; Yin, G.; Xu, L.; Wang, Y.; Wang, F.; Lu, Y. Energy-Optimal Braking Control Using a Double-Layer Scheme for Trajectory Planning and Tracking of Connected Electric Vehicles. *Chin. J. Mech. Eng.* **2021**, *34*, 83. [CrossRef]
44. International Energy Agency. *Global EV Outlook 2023: Catching Up with Climate Ambitions*; Global EV Outlook; OECD: Paris, France, 2023; ISBN 978-92-64-85692-9.
45. Page, M.J.; McKenzie, J.E.; Bossuyt, P.M.; Boutron, I.; Hoffmann, T.C.; Mulrow, C.D.; Shamseer, L.; Tetzlaff, J.M.; Akl, E.A.; Brennan, S.E.; et al. The PRISMA 2020 Statement: An Updated Guideline for Reporting Systematic Reviews. *BMJ* **2021**, *372*, n71. [CrossRef]
46. Spichartz, P.; Sourkounis, C. Brake Force Distributions Optimised with Regard to Energy Recovery for Electric Vehicles with Single Front-wheel Drive or Rear-wheel Drive. *IET Electr. Syst. Trans.* **2019**, *9*, 186–195. [CrossRef]
47. Zhao, D.; Chu, L.; Xu, N.; Sun, C.; Xu, Y. Development of a Cooperative Braking System for Front-Wheel Drive Electric Vehicles. *Energies* **2018**, *11*, 378. [CrossRef]
48. Riva, G.; Formentin, S.; Corno, M.; Savaresi, S.M. Model Predictive Control of High-Performance Braking Systems: A Force-Based Approach. *IEEE Control Syst. Lett.* **2022**, *6*, 2383–2388. [CrossRef]
49. Zhou, C.; Yu, L.; Li, Y.; Lu, Z.; Song, J. A Layered Roll Stability Control Strategy for Commercial Vehicles Based on Adaptive Model Predictive Control. *Veh. Syst. Dyn.* **2023**, *61*, 3067–3088. [CrossRef]
50. Hajiloo, R.; Khajepour, A.; Kasaiezadeh, A.; Chen, S.-K.; Litkouhi, B. A Prioritisation Model Predictive Control for Multi-Actuated Vehicle Stability with Experimental Verification. *Veh. Syst. Dyn.* **2023**, *61*, 2144–2163. [CrossRef]

51. Ma, Y.; Zhao, J.; Zhao, H.; Lu, C.; Chen, H. MPC-Based Slip Ratio Control for Electric Vehicle Considering Road Roughness. *IEEE Access* **2019**, *7*, 52405–52413. [CrossRef]
52. Huang, B.; Wu, S.; Huang, S.; Fu, X. Lateral Stability Control of Four-Wheel Independent Drive Electric Vehicles Based on Model Predictive Control. *Math. Probl. Eng.* **2018**, *2018*, 6080763. [CrossRef]
53. Zhang, Y.; Wang, W.; Yang, C.; Han, L.; Zhang, Z.; Liu, J. An Effective Regenerative Braking Strategy Based on the Combination Algorithm of Particle Swarm Optimization and Ant Colony Optimization for Electrical Vehicle. In *Proceedings of the 2019 IEEE 28th International Symposium on Industrial Electronics (ISIE)*; IEEE: Vancouver, BC, Canada, 2019; pp. 1905–1910.
54. Dong, H.; Tian, Z.; Liao, K.; Yang, J.; Spencer, J.W. Three-Stage Energy Management of Urban Rail Transit-Based Microgrid and EV Charging Station with V2T Technology. *IEEE Trans. Transp. Electrif.* **2025**, *11*, 8604–8616. [CrossRef]
55. Yu, Z.; Feng, H.; Meng, Y.; Xu, E.; Wu, Y. Braking Energy Management Strategy for Electric Vehicles Based on Working Condition Prediction. *AIP Adv.* **2022**, *12*, 015220. [CrossRef]
56. Jiang, W.; Zheng, R.; Zhang, G.; Zhu, Z.; Wang, W.; Li, C.; Tong, Q. Optimal Torque Distribution Strategy for Electric Vehicles with Electro-Hydraulic Compound Braking System. In *Proceedings of the 2023 7th CAA International Conference on Vehicular Control and Intelligence (CVCI)*; IEEE: Changsha, China, 2023; pp. 1–6.
57. Lekshmi, S.; Lal Priya, P.S. Range Extension of Electric Vehicles with Independently Driven Front and Rear PMSM Drives by Optimal Driving and Braking Torque Distribution. In *Proceedings of the 2020 IEEE International Conference on Power Electronics, Smart Grid and Renewable Energy (PESGRE2020)*; IEEE: Cochin, India, 2020; pp. 1–6.
58. You, D.; Luo, X.; Sun, Z.; Wu, H.; Wei, G.; Cheng, Y.; Gao, B. Correlation between Braking Strategy and Regenerative Braking Energy of Electric Vehicle. In *Proceedings of the 2022 41st Chinese Control Conference (CCC)*; IEEE: Hefei, China, 2022; pp. 5463–5468.
59. Wu, D.; Zhu, B.; Tan, D.; Zhang, N.; Gu, J. Multi-Objective Optimization Strategy of Adaptive Cruise Control Considering Regenerative Energy. *Proc. Inst. Mech. Eng. Part D J. Automob. Eng.* **2019**, *233*, 3630–3645. [CrossRef]
60. Aneesh, V.A.; Devadiga, S.S.; Gaurkar, P.V.; Rajesh, R.; Vivekanandan, G.; Sivaram, S.; Subramanian, S.C. High-Bandwidth Hybrid Brake Control for Enhanced Stopping of Heavy Electric Vehicles. In *Proceedings of the 2026 18th International Conference on COMmunication Systems and NETworks (COMSNETS)*; IEEE: Bengaluru, India, 2026; pp. 633–638.
61. Wang, J.; Wang, H.; Zhu, Z.; Wu, T.; Zhou, Z.; Zhao, D.; Wang, Z. Integrated Optimal Control Strategy of Electromechanical Hybrid Braking System for Four-Wheel Independent Drive/Brake Electric Vehicles. *IEEE Trans. Transp. Electrif.* **2025**, *11*, 13727–13741. [CrossRef]
62. Wu, C.-H.; Tsai, C.-L.; Yang, J.-M. Energy Management Design of Dual-Motor System for Electric Vehicles Using Whale Optimization Algorithm. *Sensors* **2025**, *25*, 4317. [CrossRef]
63. Zhang, Y.; Khajepour, A.; Hashemi, E.; Qin, Y.; Huang, Y. Reconfigurable Model Predictive Control for Articulated Vehicle Stability with Experimental Validation. *IEEE Trans. Transp. Electrif.* **2020**, *6*, 308–317. [CrossRef]
64. El-bakkouri, J.; Ouadi, H.; Giri, F.; Khafallah, M.; Gheouany, S.; Bakali, S.E. Extremum Seeking Based Braking Torque Distribution for Electric Vehicles' Hybrid Anti-Lock Braking System. *IFAC-PapersOnLine* **2023**, *56*, 2546–2551. [CrossRef]
65. Banik, I.; Nandi, A.K. Recuperative Control Strategy Based on Brake Intention Recognition in Electric Vehicles to Augment Energy Ergonomics. *J. Braz. Soc. Mech. Sci. Eng.* **2026**, *48*, 245. [CrossRef]
66. Yang, Y.; Wang, C.; Yang, S.; Tang, X. Study on Top Hierarchy Control Strategy of AEBS over Regenerative Brake and Hydraulic Brake for Hub Motor Drive BEVs. *Energies* **2022**, *15*, 8382. [CrossRef]
67. Rajamani, R. *Vehicle Dynamics and Control*; Mechanical Engineering Series; Springer: Boston, MA, USA, 2012; ISBN 978-1-4614-1432-2.
68. Dixon, J.C. *Tires, Suspension and Handling*, 2nd ed.; SAE International: Warrendale, PA, USA, 1996; ISBN 978-0-7680-6289-2.
69. Tanelli, M.; Piroddi, L.; Piuri, M.; Savaresi, S.M. Real-Time Identification of Tire-Road Friction Conditions. *IET Control Theory Appl.* **2009**, *3*, 891–906. [CrossRef]
70. Li, W.; Li, H.; Huang, Z.; Liu, J.; Dang, S.; Du, H. A New Braking Torque Distribution Strategy Based on Braking Actuator Characteristics and a Command Signal for a Blended Braking System. *IET Intell. Trans. Sys.* **2022**, *16*, 825–841. [CrossRef]
71. Qi, G.; Yue, M.; Xu, M.; Zhang, L.; Liu, Y. Integrated NMPC-Based Vehicle Stability and Tracking Control Strategy for Heavy-Duty Truck with Road Bank Angle Estimation. *J. Vib. Control* **2025**. [CrossRef]
72. Zheng, Z.; Wang, S.; Zhao, X.; Yu, Q.; Zhang, H.; Lv, Y.; Tian, J. Adaptive Model Predictive Control of Four-Wheel Drive Intelligent Electric Vehicles Based on Stability Probability Under Extreme Braking Conditions. *IEEE Trans. Intell. Veh.* **2024**, *11*, 618–628. [CrossRef]
73. Kennedy, J.; Eberhart, R. Particle Swarm Optimization. In *Proceedings of the Proceedings of ICNN'95—International Conference on Neural Networks*; IEEE: Perth, WA, Australia, 1995; Volume 4, pp. 1942–1948.
74. Kissai, M.; Monsuez, B.; Mouton, X.; Martinez, D.; Tapus, A. Model Predictive Control Allocation of Systems with Different Dynamics. In *Proceedings of the 2019 IEEE Intelligent Transportation Systems Conference (ITSC)*; IEEE: Auckland, New Zealand, 2019; pp. 4170–4177.

75. Georgiev, P.; De Filippis, G.; Gruber, P.; Sorniotti, A. On the Benefits of Active Aerodynamics on Energy Recuperation in Hybrid and Fully Electric Vehicles. *Energies* **2023**, *16*, 5843. [CrossRef]
76. Hajiloo, R.; Khajepour, A.; Kasaiezadeh, A.; Chen, S.-K.; Litkouhi, B. A Model Predictive Control of Electronic Limited Slip Differential and Differential Braking for Improving Vehicle Yaw Stability. *IEEE Trans. Contr. Syst. Technol.* **2023**, *31*, 797–808. [CrossRef]
77. Yang, H.; Lin, H.; Fang, S.; Huang, Y.; Zhu, Z.Q. Novel Partitioned Stator Hybrid Magnet Memory Machines for EV/HEV Applications. In *Proceedings of the 2016 IEEE Vehicle Power and Propulsion Conference (VPPC)*; IEEE: Hangzhou, China, 2016; pp. 1–6.
78. Li, Y.; Zhao, C.; Huang, Y.; Wang, X.; Guo, F.; Yang, L. Study on Regenerative Braking Control Strategy for Extended Range Electric Vehicles. In *Proceedings of the 2020 IEEE Vehicle Power and Propulsion Conference (VPPC)*; IEEE: Gijon, Spain, 2020; pp. 1–6.
79. Zhang, B.; Wang, Z.; Yang, Z.; Zhou, N.; Chen, Z. Integrated Braking Control for Electric Vehicles Toward Enhanced Energy Recovery and Dynamic Stability. *Int. J. Automot. Technol.* **2026**. [CrossRef]
80. Rawlings, J.B.; Mayne, D.Q.; Diehl, M.M. *Model Predictive Control: Theory, Computation, and Design*, 2nd ed.; Nob Hill Publishing, LLC: Madison, WI, USA, 2024.
81. Camacho, E.F.; Bordons, C.; Maestre, J.M. *Model Predictive Control*; Advanced Textbooks in Control and Signal Processing; Springer: Cham, Switzerland, 2026; ISBN 978-3-031-87595-3.
82. Poli, R.; Kennedy, J.; Blackwell, T. Particle Swarm Optimization: An Overview. *Swarm Intell.* **2007**, *1*, 33–57. [CrossRef]
83. Shi, Y.; Eberhart, R. A Modified Particle Swarm Optimizer. In *Proceedings of the 1998 IEEE International Conference on Evolutionary Computation Proceedings; IEEE World Congress on Computational Intelligence (Cat. No.98TH8360)*; IEEE: Anchorage, AK, USA, 1998; pp. 69–73.
84. He, Y.; Fan, S.; Hyun Kwak, K.; Kim, Y. Personalized Automated Braking for One-Pedal Driving in Electric Vehicles Using Model Predictive Control. *IEEE Trans. Transp. Electrif.* **2025**, *11*, 3215–3228. [CrossRef]

Disclaimer/Publisher's Note: The statements, opinions and data contained in all publications are solely those of the individual author(s) and contributor(s) and not of MDPI and/or the editor(s). MDPI and/or the editor(s) disclaim responsibility for any injury to people or property resulting from any ideas, methods, instructions or products referred to in the content.